MEMORANDUM REPORT BRL-MR-3733

BRL

1938 – Serving the Army for Fifty Years – 1988

THE AERODYNAMIC CHARACTERISTICS OF 7.62MM MATCH BULLETS

ROBERT L. McCOY

DECEMBER 1988

U.S. ARMY LABORATORY COMMAND

BALLISTIC RESEARCH LABORATORY

ABERDEEN PROVING GROUND, MARYLAND

UNCLASSIFIED

SECURITY CLASSIFICATION OF THIS PAGE

REPORT DOCUMENTATION PAGE

Form Approved
OMB No. 0704-0188

1a. REPORT SECURITY CLASSIFICATION UNCLASSIFIED	1b. RESTRICTIVE MARKINGS
2a. SECURITY CLASSIFICATION AUTHORITY	3. DISTRIBUTION/AVAILABILITY OF REPORT Approved for public release; distribution is unlimited
2b. DECLASSIFICATION/DOWNGRADING SCHEDULE	
4. PERFORMING ORGANIZATION REPORT NUMBER(S) BRL-MR-3733	5. MONITORING ORGANIZATION REPORT NUMBER(S)
6a. NAME OF PERFORMING ORGANIZATION US Army Ballistic Research Laboratory 6b. OFFICE SYMBOL (If applicable) SLCBR-LF	7a. NAME OF MONITORING ORGANIZATION
6c. ADDRESS (City, State, and ZIP Code) Aberdeen Proving Ground, MD 21005-5066	7b. ADDRESS (City, State, and ZIP Code)
8a. NAME OF FUNDING/SPONSORING ORGANIZATION US Army Ballistic Research Laboratory 8b. OFFICE SYMBOL (If applicable) SLCBR-DD-T	9. PROCUREMENT INSTRUMENT IDENTIFICATION NUMBER
8c. ADDRESS (City, State, and ZIP Code) Aberdeen Proving Ground, MD 21005-5066	10. SOURCE OF FUNDING NUMBERS PROGRAM ELEMENT NO. 62618A PROJECT NO. 1L1 62618AH80 TASK NO. WORK UNIT ACCESSION NO.

11. TITLE (Include Security Classification)

The Aerodynamic Characteristics of 7.62mm Match Bullets

12. PERSONAL AUTHOR(S)
McCOY, ROBERT L.

13a. TYPE OF REPORT	13b. TIME COVERED FROM _____ TO _____	14. DATE OF REPORT (Year, Month, Day)	15. PAGE COUNT

16. SUPPLEMENTARY NOTATION

17. COSATI CODES			18. SUBJECT TERMS (Continue on reverse if necessary and identify by block number)	
FIELD	GROUP	SUB-GROUP	7.62mm Match Bullets	Gyroscopic Stability
01	01		Aerodynamic Characteristics	Dynamic Stability
			Aerodynamic Drag	Yaw Limit-Cycle

19. ABSTRACT (Continue on reverse if necessary and identify by block number)

Spark photography range tests of three 7.62mm match bullets were conducted to determine the aerodynamic and flight dynamic characteristics at supersonic and subsonic speeds. The drag coefficients of the match bullets were determined, and recommendations for rifling twist rates to insure gyroscopic stability were made. The observed nonlinear Magnus moment properties of the 7.62mm match bullets predict a small slow arm limit cycle yaw at supersonic speeds, and a larger limit cycle yaw at subsonic speeds.

20. DISTRIBUTION/AVAILABILITY OF ABSTRACT	21. ABSTRACT SECURITY CLASSIFICATION
☐ UNCLASSIFIED/UNLIMITED ☒ SAME AS RPT ☐ DTIC USERS	UNCLASSIFIED

22a. NAME OF RESPONSIBLE INDIVIDUAL	22b TELEPHONE (Include Area Code)	22c. OFFICE SYMBOL
ROBERT L. McCOY	301-278-3880	SLCBR-LF-T

DD Form 1473, JUN 86 *Previous editions are obsolete.*

SECURITY CLASSIFICATION OF THIS PAGE
UNCLASSIFIED

Table of Contents

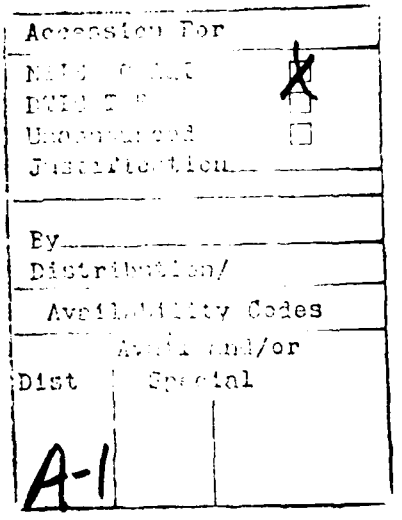

List of Figures

List of Figures (Continued)

List of Tables

I. Introduction

The marksmanship training units of the various U.S. Armed Services have traditionally been interested in the ballistics of national match rifles and ammunition. The Ballistic Research Laboratory (BRL) has received many questions over the years concerning match ammunition performance, from captains of service rifle teams, marksmanship training instructors, and U.S. Olympic match shooters. The answers provided in the past by the BRL were best estimates, since no aeroballistic data had ever been collected for match ammunition.

The first BRL spark photography range firings of a match bullet were conducted in 1975, using the 7.62mm, 168 grain Sierra International bullet, fired from a Remington 40-XB match rifle chambered for 7.62mm NATO (.308 Winchester). The 168 grain Sierra International is a commercial match bullet, which is currently loaded in the M852 Match ammunition. Additional spark range tests were conducted in 1980, to extend the data base for the 168 grain Sierra International bullet, and to determine the aeroballistic properties of the 7.62mm M118 Match (Special Ball) ammunition, and the 190 grain Sierra Matchking Hollow Point bullet.

This report is a consolidation of all the BRL aeroballistic data collected for 7.62mm match bullets from 1975 to the present.

II. Test Facilities and Material

The spark range firings were conducted in the BRL Free Flight Aerodynamics Range. [1] The Aerodynamics Range is an enclosed, instrumented firing range designed to accurately record the flight of a projectile over approximately 90 metres of its trajectory. The free flight range technique for obtaining aerodynamic data demands unusually high accuracy in the measurement of position, time of flight, and projectile pitch and yaw angles. Figure 1 is a photograph (circa 1958) of the BRL Free Flight Aerodynamics Range. Figure 2 is a schematic illustration of the coordinate reference system for the range.

The 1975 firings of the 168 grain Sierra International bullet were conducted using a Remington Model 40-XB "Rangemaster" Center Fire Rifle, chambered in .308 Winchester, with a 27.25 inch barrel, and a rifling twist rate of 1 turn in 12 inches. Launch Mach numbers varied from 2.2 down to 1.4, and yaw levels from 1 degree to 7 degrees were induced using a half-muzzle yaw inducer with a variable lip extension. For the 1980 firings of the M118 Match and the 190 grain Sierra Matchking bullets, a Remington Model 700 ADL rifle chambered in .308 Winchester was used. The Model 700 barrel length was 22 inches, and rifling twist rate was 1 turn in 10 inches. The faster twist rifling was used for the 1980 tests because preliminary calculations had indicated that the gyroscopic stability of the heavier bullets might be too low at subsonic launch velocities, from the 12 inch twist barrel used in 1975.

Launch Mach numbers for the 1980 tests varied from 2.2 down to 0.6, so the entire useful velocity range of the match bullets would be covered. For completeness, the 168 grain Sierra International bullets were also tested at low supersonic and subsonic speeds. Yaw levels induced in the 1980 tests were essentially the same as those obtained in 1975.

All firings used Lake City Match cartridge cases, and appropriate charges of IMR 4895 propellant were used for the higher supersonic speeds. Reduced charges of IMR 4198 propellant were used for the lower supersonic velocities. Further reduced charges of Hercules 2400 and Hercules UNIQUE were used to achieve the desired subsonic speeds. Figures 3 through 5 are sketches of the three match bullets tested. A sample of five each of the three projectile types were measured for complete physical characteristics. The average physical properties of the match bullets are presented in Table 1.

III. Results

The free flight spark range data were fitted to solutions of the linearized equations of motion and the resulting flight motion parameters were used to infer linearized aerodynamic coefficients, using the methods of Reference 2. Preliminary analysis of the aerodynamic data showed distinct variation of several coefficients with yaw level. In BRL Report 974, Murphy [3] has shown that aerodynamic coefficients derived from the linearized data reduction can be used to infer the coefficients in a nonlinear force and moment expansion, if sufficient data are available. For the 7.62mm match bullets, sufficient data were obtained to permit determination of several nonlinear aerodynamic coefficients. A more detailed analysis of nonlinear effects is presented in the subtopics of this section, which discuss individual aerodynamic coefficients.

An interesting and useful by-product of spark photography range testing is the high quality shadowgraph information obtained. Figures 6 through 17 show the flowfields around the three 7.62mm match bullets at four supersonic Mach numbers. The shadowgraph figures were selected from range stations where the angle of attack was less than one degree.

The round-by-round aerodynamic data obtained for the 7.62mm match bullets are listed in Tables 2, 3 and 4. Free flight motion parameters for the three bullets are listed in Tables 5, 6 and 7.

1. Drag Coefficient

The drag coefficient, C_D, is determined by fitting the time-distance measurements from the range flight. C_D is distinctly nonlinear with yaw level, and the value determined from an individual flight reflects both the zero-yaw drag coefficient, C_{D_0}, and the induced

drag due to the average yaw level of the flight. The drag coefficient variation is expressed as an even power series in yaw amplitude:

$$C_D = C_{D_0} + C_{D_{\delta^2}} \delta^2 + \ldots \quad (1)$$

where C_{D_0} is the zero-yaw drag coefficient $C_{D_{\delta^2}}$ is the quadratic yaw drag coefficient, and δ^2 is the total angle of attack squared.

Analysis of the zero-yaw drag coefficient data for the 7.62mm match bullets showed that the M118 bullet had the lowest drag of the three designs tested, at supersonic speeds. The 190 grain Sierra Matchking averaged four percent higher drag than the M118, and the 168 grain Sierra International bullet averaged eight percent higher drag than the military M118 design, over the Mach number range 2.2 to 1.1. At subsonic speeds, the zero-yaw drag coefficients of the three bullets are nearly identical. Figures 18, 19 and 20 show the variation of zero-yaw drag coefficient with Mach number for the three match bullets tested. The variation of the quadratic yaw drag coefficients, $C_{D_{\delta^2}}$, with Mach number are shown in Figures 21, 22 and 23, for the respective bullet designs. The yaw drag coefficients presented were used to correct the range measured total drag coefficients to zero-yaw values. Dashed portions of curves are used throughout this report to indicate trends, in regions where no data were collected.

The round-to-round standard deviation in zero-yaw drag coefficient at supersonic speeds was determined for each match bullet design, from the least-squares fit of the drag data. All the 7.62mm match bullets showed standard deviations in C_{D_0} between 0.7 percent and 0.8 percent, which represents significant improvement over the one to three percent drag standard deviations typical of military ball projectiles. The standard deviation in drag coefficient for an individual flight in the BRL Aerodynamics Range is of order of 0.2 percent, hence the measurement error does not contribute significantly to the observed round-to-round standard deviation in drag.

2. Overturning Moment Coefficient

The range values of the overturning moment coefficient, C_{M_α}, were fitted using the appropriate squared-yaw parameters from Reference 3. A weak dependence of C_{M_α} on yaw level was observed for all the 7.62mm match bullets. The overturning moment is assumed to be cubic in yaw level, and the coefficient variation is given by:

$$C_{M_\alpha} = C_{M_{\alpha 0}} + C_2 \delta^2 + \ldots \quad (2)$$

where $C_{M_{\alpha_0}}$ is the zero-yaw overturning moment coefficient, and C_2 is the cubic coefficient.

The variation of $C_{M_{\alpha_0}}$ with Mach number for the three 7.62mm match bullets is shown in Figures 24 through 26. The cubic overturning moment coefficients, C_2, used to correct the range values of C_{M_α} to zero-yaw conditions, are included on the figures.

3. Gyroscopic Stability

The variation of launch gyroscopic stability factor, S_g, with launch Mach number, at standard atmospheric conditions, is shown for the three 7.62mm match bullets in Figures 27 through 29. The stability factors for 10 inch twist and 12 inch twist of rifling are illustrated. For a launch Mach number of 2.3 (muzzle velocity approximately 2570 feet/second), the M118 bullet from a 12 inch twist barrel has a gyroscopic stability factor of 1.4; the stability factor of the 190 grain Sierra Matchking at the same muzzle velocity and twist rate is 1.3. The corresponding value of S_g for the 168 grain Sierra International bullet at the same conditions is 1.65. Thus all the above 7.62mm match bullets are gyroscopically stable when fired from a 12 inch twist barrel at muzzle velocities greater than 2500 feet/second. However, for the M118 bullet, and especially for the 190 grain Sierra Matchking, there is no margin of safety for cold weather (high air density) atmospheric conditions, if a 12 inch twist is selected.

A launch gyroscopic stability factor between 1.5 and 2.0 is usually specified, to insure ample safety margin under worst case conditions. Thus for the 7.62mm NATO cartridge, the 12 inch twist rate is an excellent choice for the 168 grain Sierra International (M852) bullet, and a 10 inch twist barrel should be selected for the M118 or 190 grain Sierra Matchking bullets.

4. Lift Force Coefficient

The range values of the lift force coefficient, C_{L_α}, were also analyzed using the methods of Reference 3. No significant value of the cubic lift force coefficient could be found, for any of the three 7.62mm match bullets. The range values of the lift force coefficient are plotted against Mach number in Figure 30.

No significant difference in lift force coefficient with bullet type is observed in Figure 30. The curve in the plot was obtained from a least squares fit of the C_{L_α} data, and should be used for all three 7.62mm match bullets. The lift force coefficient is not as well determined from spark range tests as is the overturning moment coefficient. This fact is reflected in the larger round-to-round data scatter observed in Figure 30, compared with the overturning moment coefficient data plotted in Figures 24 through 26.

5. Magnus Moment Coefficient and Pitch Damping Moment Coefficient

The Magnus moment coefficient, $C_{M_{p\alpha}}$, and the pitch damping moment coefficient, $(C_{M_q} + C_{M_{\dot{\alpha}}})$, are discussed together, since if either coefficient is nonlinear with yaw level, both coefficients exhibit nonlinear coupling in the data reduction process. [3] Due to mutual reaction, the analysis of $C_{M_{p\alpha}}$ and $(C_{M_q} + C_{M_{\dot{\alpha}}})$ must be performed simultaneously, although the aerodynamic moments are not, in themselves, directly physically related.

If the dependence of the Magnus moment and the pitch damping moment are cubic in yaw level, the nonlinear variation of the two moment coefficients is of the general form:

$$C_{M_{p\alpha}} = C_{M_{p\alpha 0}} + \hat{C}_2 \, \delta^2 \tag{3}$$

$$\left(C_{M_q} + C_{M_{\dot{\alpha}}}\right) = \left(C_{M_q} + C_{M_{\dot{\alpha}}}\right)_0 + d_2 \, \delta^2 \tag{4}$$

where $C_{M_{p\alpha 0}}$ and $\left(C_{M_q} + C_{M_{\dot{\alpha}}}\right)_0$ are the zero-yaw values of Magnus and pitch damping moment coefficients, respectively, and $\hat{C}_2$ and d_2 are the associated cubic coefficients.

In Reference 3, it is shown that the non-linear coupling introduced through the data reduction yields the following expressions for range values [R-subscript] of $C_{M_{p\alpha}}$ and $\left(C_{M_q} + C_{M_{\dot{\alpha}}}\right)$:

$$\left[C_{M_{p\alpha}}\right]_R = C_{M_{p\alpha 0}} + \hat{C}_2 \, \delta_e^2 + d_2 \, \delta_{e_{TH}}^2 \tag{5}$$

$$\left[\left(C_{M_q} + C_{M_{\dot{\alpha}}}\right)\right]_R = \left(C_{M_q} + C_{M_{\dot{\alpha}}}\right)_0 + \hat{C}_2 \, \delta_{e_{HT}}^2 + d_2 \, \delta_{e_{HH}}^2 \tag{6}$$

where the above effective squared yaws are defined as:

$$\delta_e^2 = K_F^2 + K_S^2 + \frac{(\phi'_F \, K_F^2 - \phi'_S \, K_S^2)}{(\phi'_F - \phi'_S)} \tag{7}$$

$$\delta_{e_{TH}}^2 = \left(\frac{I_x}{I_y}\right)\left[\frac{(K_F^2 \, \phi'^2_F - K_S^2 \, \phi'^2_S)}{(\phi'^2_F - \phi'^2_S)}\right] \tag{8}$$

$$\delta_{e_{HT}}^2 = \left(\frac{I_y}{I_x}\right)\left[\frac{(\phi'_F + \phi'_S)\,(K_S^2 - K_F^2)}{(\phi'_F - \phi'_S)}\right] \tag{9}$$

$$\delta_{e_{HH}}^2 = \frac{(\phi'_F \, K_S^2 - \phi'_S \, K_F^2)}{(\phi'_F - \phi'_S)} \tag{10}$$

The remaining symbols are defined in the List of Symbols in this report.

Preliminary analysis of the 7.62mm match bullet data showed strong nonlinearity in the range values of $C_{M_{p\alpha}}$ and $(C_{M_q} + C_{M_{\dot{\alpha}}})$ at angles of attack less than 2 degrees, for both supersonic and subsonic speeds. The data rounds were separated into Mach number groups, by bullet type, and an analysis was performed to determine the cubic coefficients at both small and large yaw levels. No significant values of the cubic pitch damping moment coefficient, d_2, could be found.

The data were then analyzed assuming a cubic Magnus moment and linear pitch damping moment. Further analysis revealed no significant variation of either coefficient with bullet type at supersonic speeds, and all bullet types were then combined for final analysis.

The combined data rounds were again separated into Mach number groups, and final values of the cubic Magnus moment coefficient were obtained. Plots of the range Magnus moment coefficient versus $\delta_e{}^2$ are shown in Figures 31 through 34, for the four Mach number intervals selected.

The Magnus moments of the 7.62mm match bullets show a bi-cubic behavior; i.e., a strong cubic dependence on angle of attack at small yaw level, followed by a very weak dependence on angle of attack at larger yaw levels. The small yaw cubic Magnus moment coefficient, $\hat{C}_2$, appears to be constant for all bullet types at all supersonic speeds, and has the value $\hat{C}_2 = 250$. The angle of attack at which bi-cubic behavior begins increases slowly with decreasing Mach number; at $M = 2$ the critical angle of attack is around 2 degrees, and at $M = 1.1$ the critical angle has increased to about 4 degrees. At subsonic speeds the value of $\hat{C}_2 = 300$ was obtained, and bi-cubic behavior appears at angles of attack of approximately 5 degrees. A significant variation of the Magnus moment with bullet type is also observed at subsonic speeds, as is illustrated in Figure 34.

The cubic Magnus moment coefficients were then used to correct the range values of $C_{M_{p\alpha}}$ and $(C_{M_q} + C_{M_{\dot{\alpha}}})$ to zero-yaw conditions, and the results are illustrated in Figures 35 through 38. A comparison of Figures 35 and 36 shows that the three 7.62mm match bullets have essentially identical zero-yaw Magnus moment coefficients at supersonic speeds, but the 168 grain Sierra International bullet shows 50 percent larger (negative) coefficients than the other bullets, at subsonic speeds. The pitch damping moment coefficients, corrected to zero-yaw conditions, are shown in Figures 37 and 38. The effect of bullet type on the pitch damping moment at subsonic speeds is even more startling than that observed for the Magnus moment. The average value of $\left(C_{M_q} + C_{M_{\dot{\alpha}}}\right)_0$ for the M118 and the 190 grain Sierra Matchking bullets at subsonic speeds is approximately -4; the 168 grain Sierra bullet shows three out of four values positive, with an average zero-yaw pitch damping moment coefficient of $+1$.

It should be noted that the analysis of nonlinear Magnus and pitch damping data from free flight spark ranges is a delicate process at best, and the results are highly sensitive to small errors in determination of the damping exponents on the two modal arms. The uncertainties in damping rate determinations are reflected in the larger round-to-round data scatter in Magnus and pitch damping moment coefficients, compared with the smaller scatter observed in the overturning moment coefficients.

6. Damping Rates

The damping rates, λ_F and λ_S, of the fast and slow yaw modes indicate the dynamic stability of a projectile. Negative λ's indicate damping; a positive λ means that its associated modal arm will grow with increasing distance along the trajectory.

For a projectile whose Magnus or pitch damping moments are nonlinear with yaw level, the damping rates also show a nonlinear dependence on yaw. [4] Figures 39 through 42 illustrate the variations in damping rates with yaw level for the 7.62mm match bullets at supersonic and subsonic speeds.

At supersonic speeds, the fast arm is always damped, for all the bullet types, at all yaw levels tested. The slow arm is undamped at small yaw levels, but damped at larger yaw. Thus a slow arm limit cycle yaw is predicted at supersonic speeds; the expected magnitude is about 2 degrees.

At subsonic speeds, the fast arm is damped at all yaw levels for the M118 and 190 grain Sierra Matchking bullets. The fast arm for the 168 grain Sierra International bullet is essentially neutrally damped at small yaw, and is probably damped at larger yaw levels, although no data were taken to substantiate this estimate. The slow arm at subsonic speeds shows the same characteristic behavior observed at supersonic speeds; dynamically unstable at small yaw, but stable at larger yaw levels. The predicted magnitude of the slow arm limit cycle yaw at subsonic speeds is approximately 4.5 degrees for the M118 and 190 grain Sierra Matchking bullets, and about five degrees for the 168 grain Sierra International (M852) bullet.

No direct measurement of limit cycle yaw at long range has been made for any of the 7.62mm match bullets. However, a two degree limit cycle yaw at supersonic speeds and a four to five degree limit cycle yaw at subsonic speeds are consistent with unpublished results obtained by Piddington for the similarly shaped 7.62mm, Ball M80 bullet, and with results obtained by the author for 5.56mm M855 and SS-109 bullets. [5]

IV. Conclusions

The M118 Match (Special Ball) bullet has the lowest drag coefficient of the three 7.62mm match bullets tested, at supersonic speeds. The 190 grain Sierra Matchking bullet shows four percent higher average drag coefficient than the M118, and the 168 grain Sierra International (M852) bullet shows eight percent higher average drag coefficient than the M118 design.

The round-to-round variation in drag coefficient for the 7.62mm match bullets is significantly smaller than that observed for typical military ball bullets. The standard deviation in C_{D_0} for the match bullets, at supersonic speeds, was found to be between 0.7 percent and 0.8 percent.

The three 7.62mm match bullets, launched at standard atmospheric conditions and at muzzle velocities above 2500 feet per second, are gyroscopically stable from a 12 inch twist of rifling. To insure an adequate margin of safety for cold weather (high air density) conditions, a 10 inch twist rate should be selected for the M118 and 190 grain Sierra Matchking bullets.

The nonlinear Magnus moment properties of the 7.62mm match bullets predict a slow arm limit cycle yaw of approximately two degrees at supersonic speeds, growing to four

to five degrees at subsonic speeds. Although the predicted limit cycle yaws are consistent with observations made for similarly shaped bullets, the long range flight dynamic results need to be verified by an independent experiment.

V. Recommendations

It is recommended that a 12 inch twist of rifling be selected for firing the 168 grain Sierra International (M852) bullet from the 7.62mm NATO cartridge case. A 10 inch twist of rifling should be selected for the M118 or 190 grain Sierra Matchking bullets, to allow a cold weather safety margin.

A long range limit cycle yaw test should be conducted with 7.62mm match bullets, to verify the flight dynamic predictions made in this report.

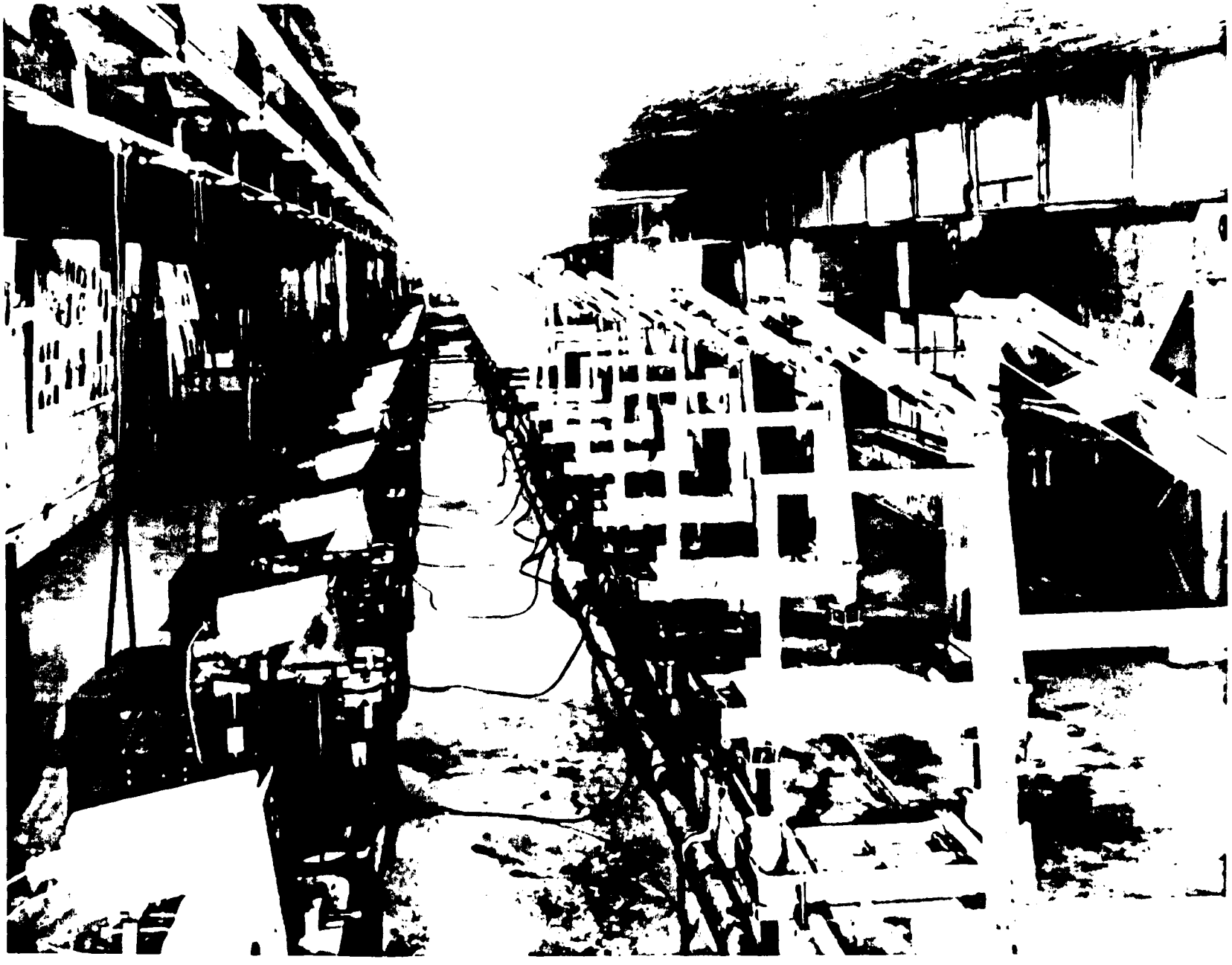

Figure 1. Photograph of the BRL Free Flight Aerodynamics Range.

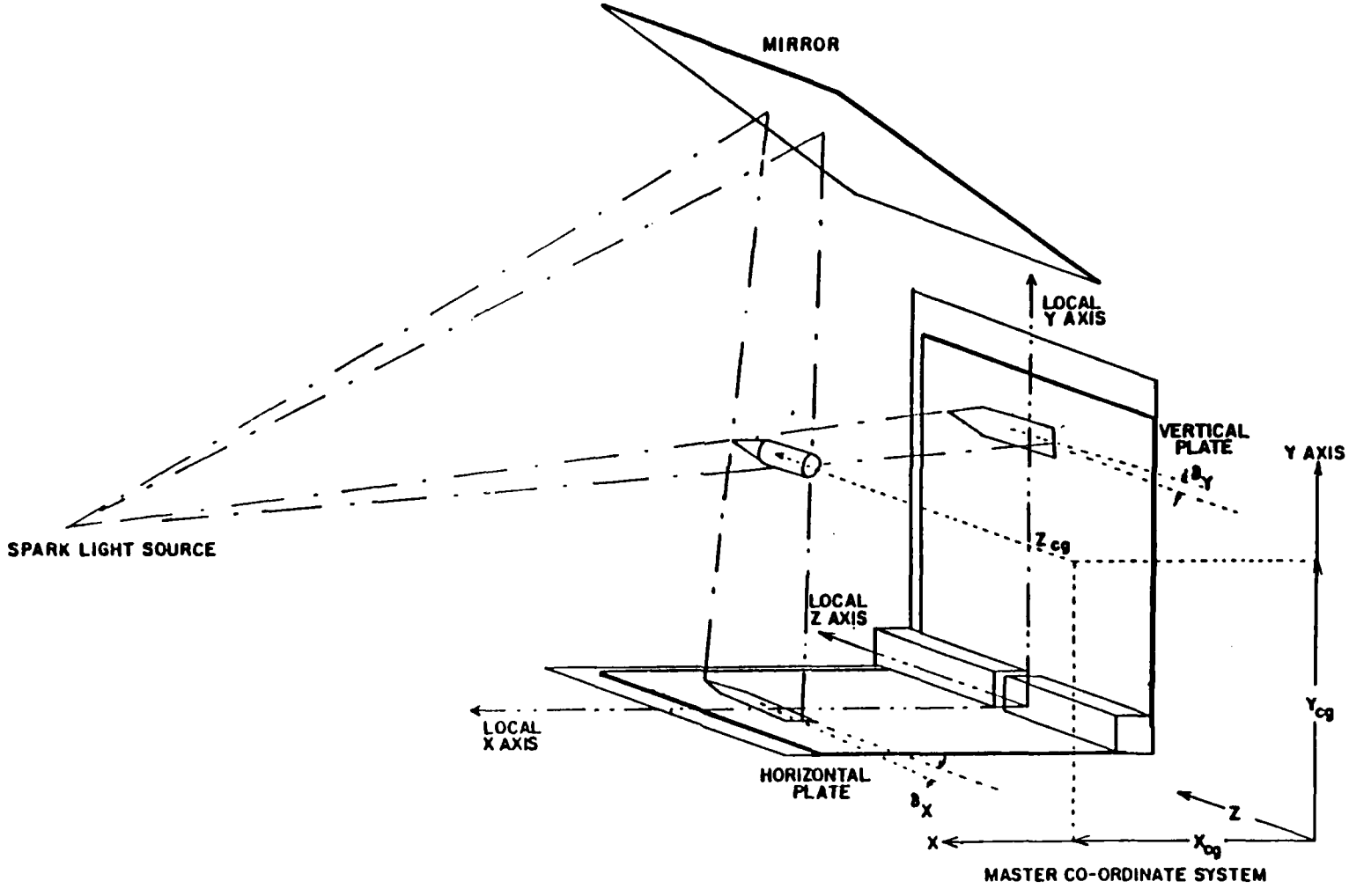

Figure 2. Coordinate System for the BRL Aerodynamics Range.

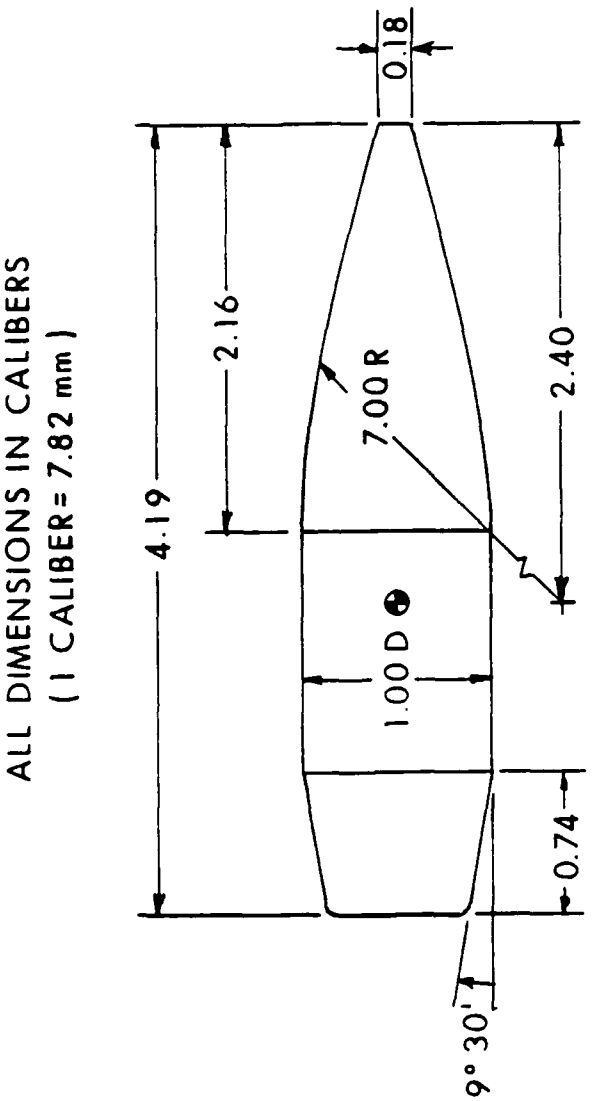

Figure 3. Sketch of the M118 Match (Special Ball) Bullet.

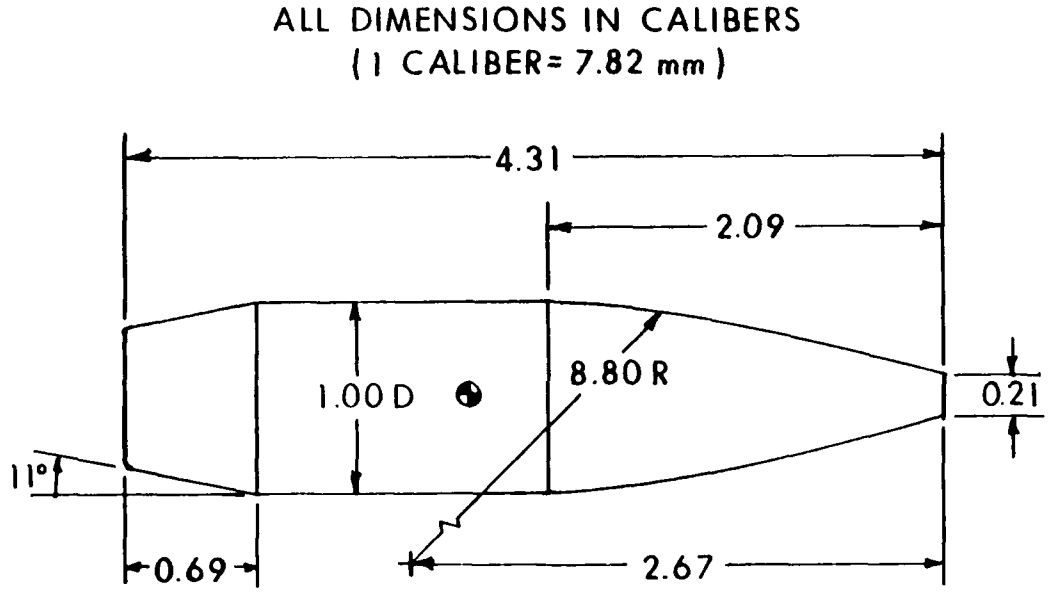

Figure 4. Sketch of the 190 Grain Sierra Matchking Bullet.

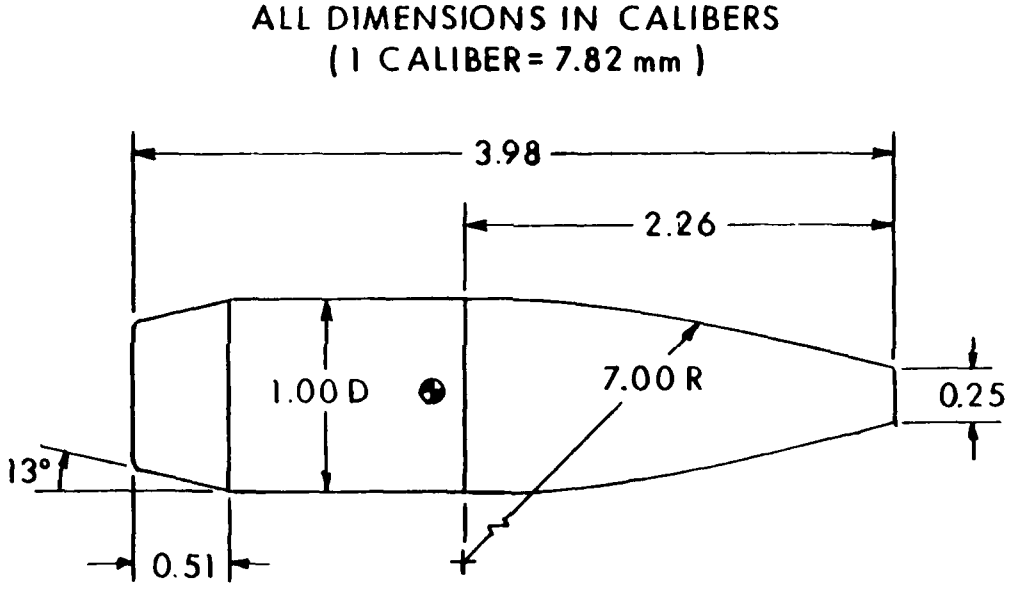

Figure 5. Sketch of the 168 Grain Sierra International (M852) Bullet.

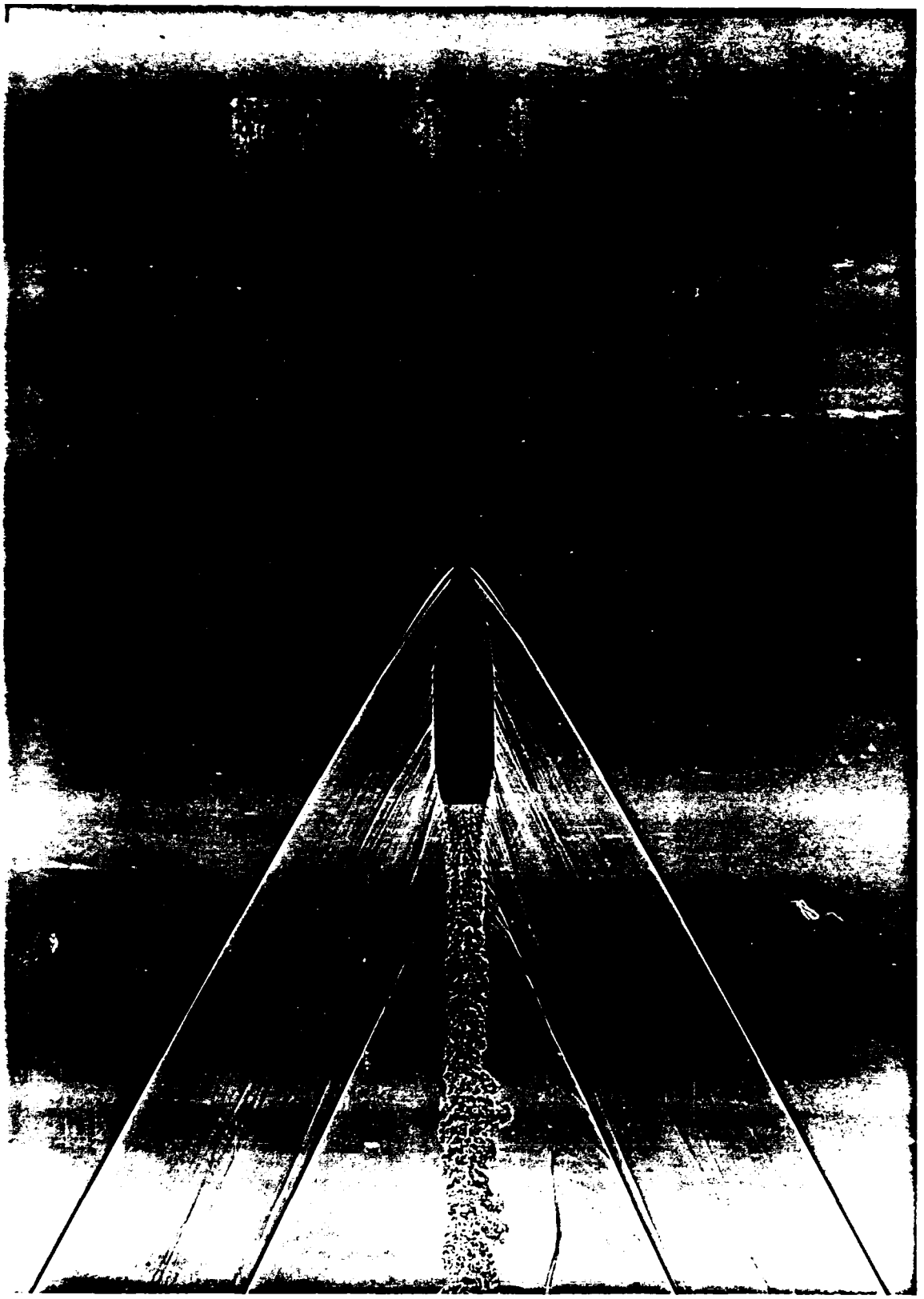

Figure 6. Shadowgraph of M118 Bullet at Mach 2.2.

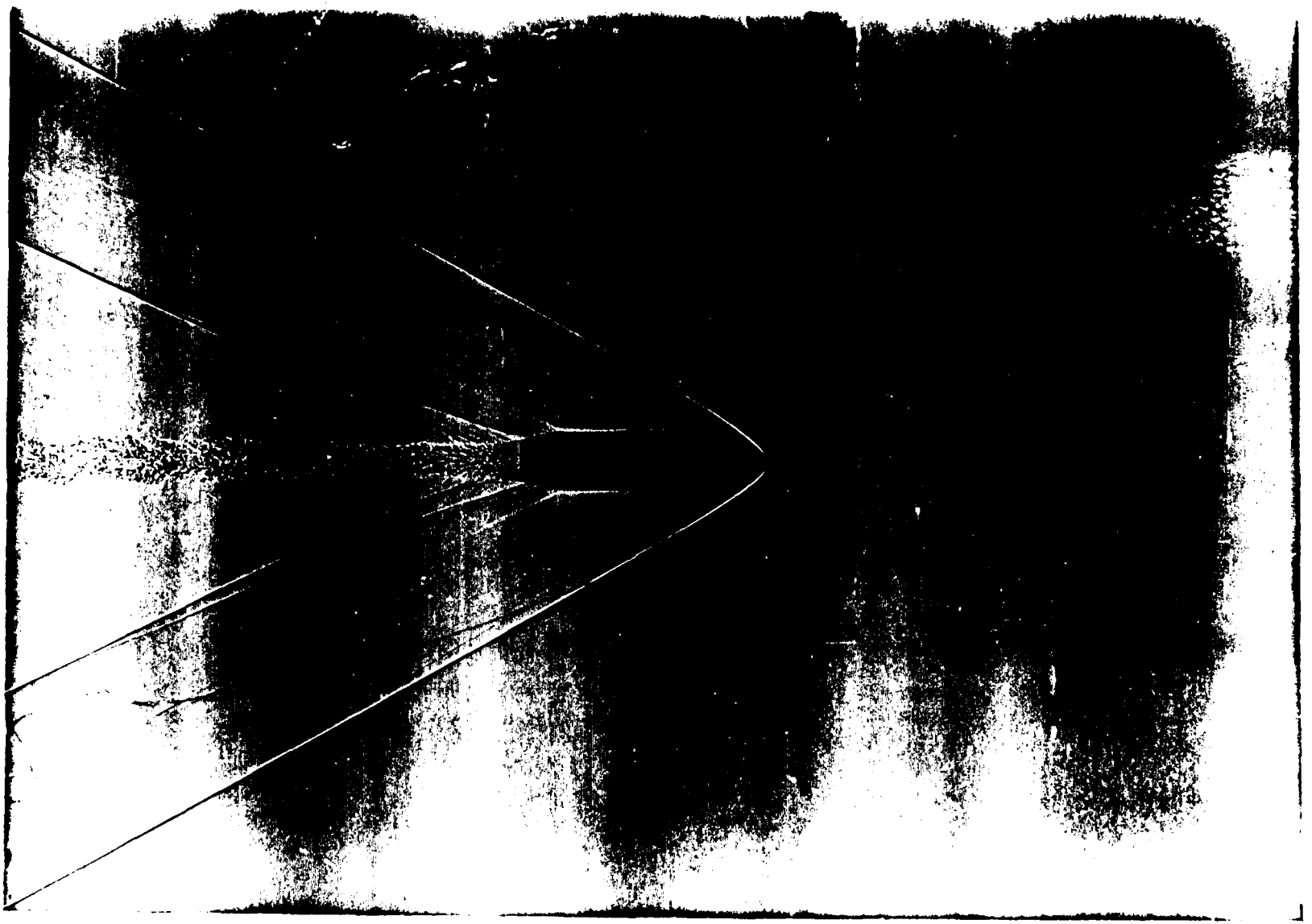

Figure 7. Shadowgraph of 190 Grain Sierra Bullet at Mach 2.2.

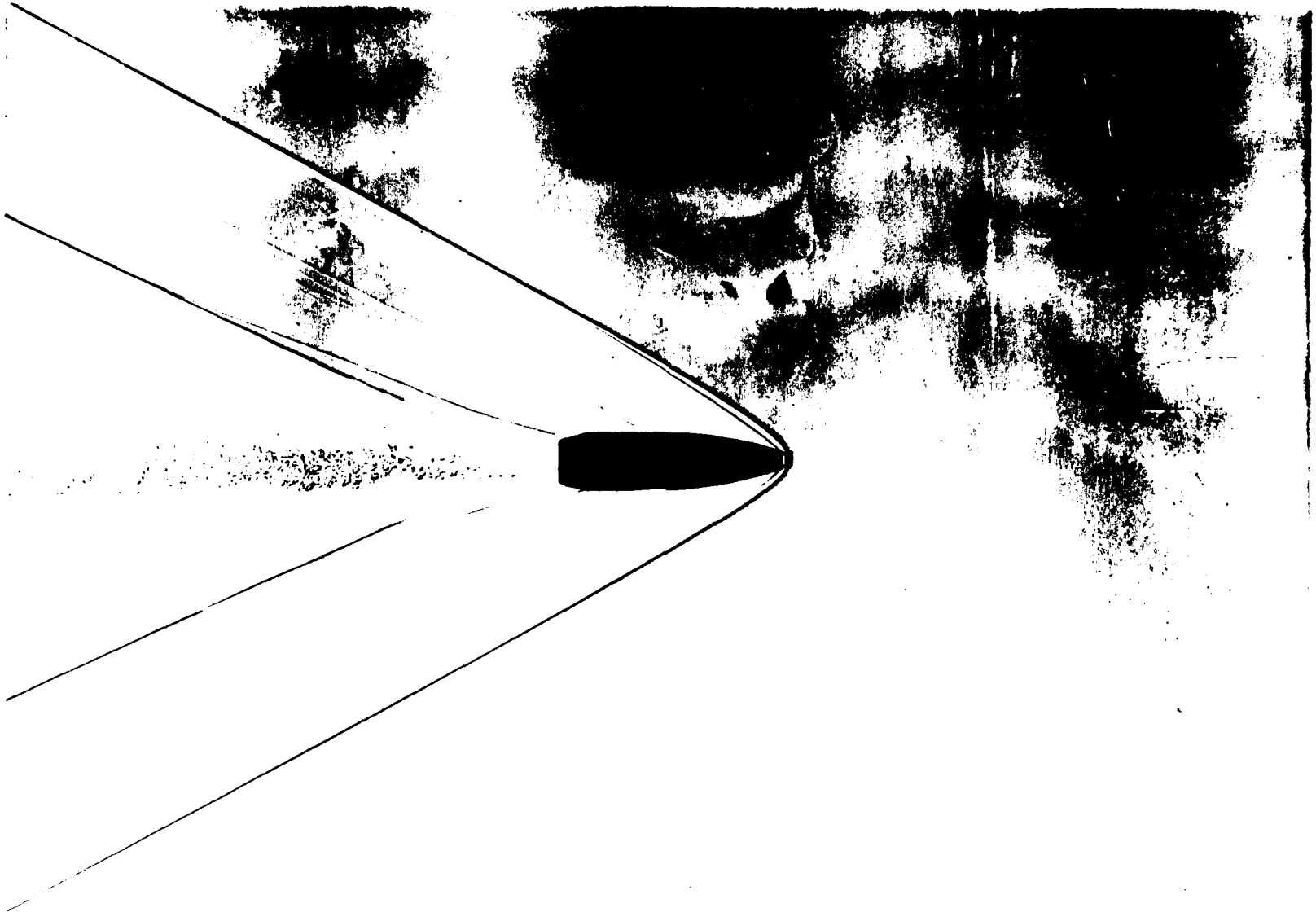

Figure 8. Shadowgraph of 168 Grain Sierra Bullet at Mach 2.2.

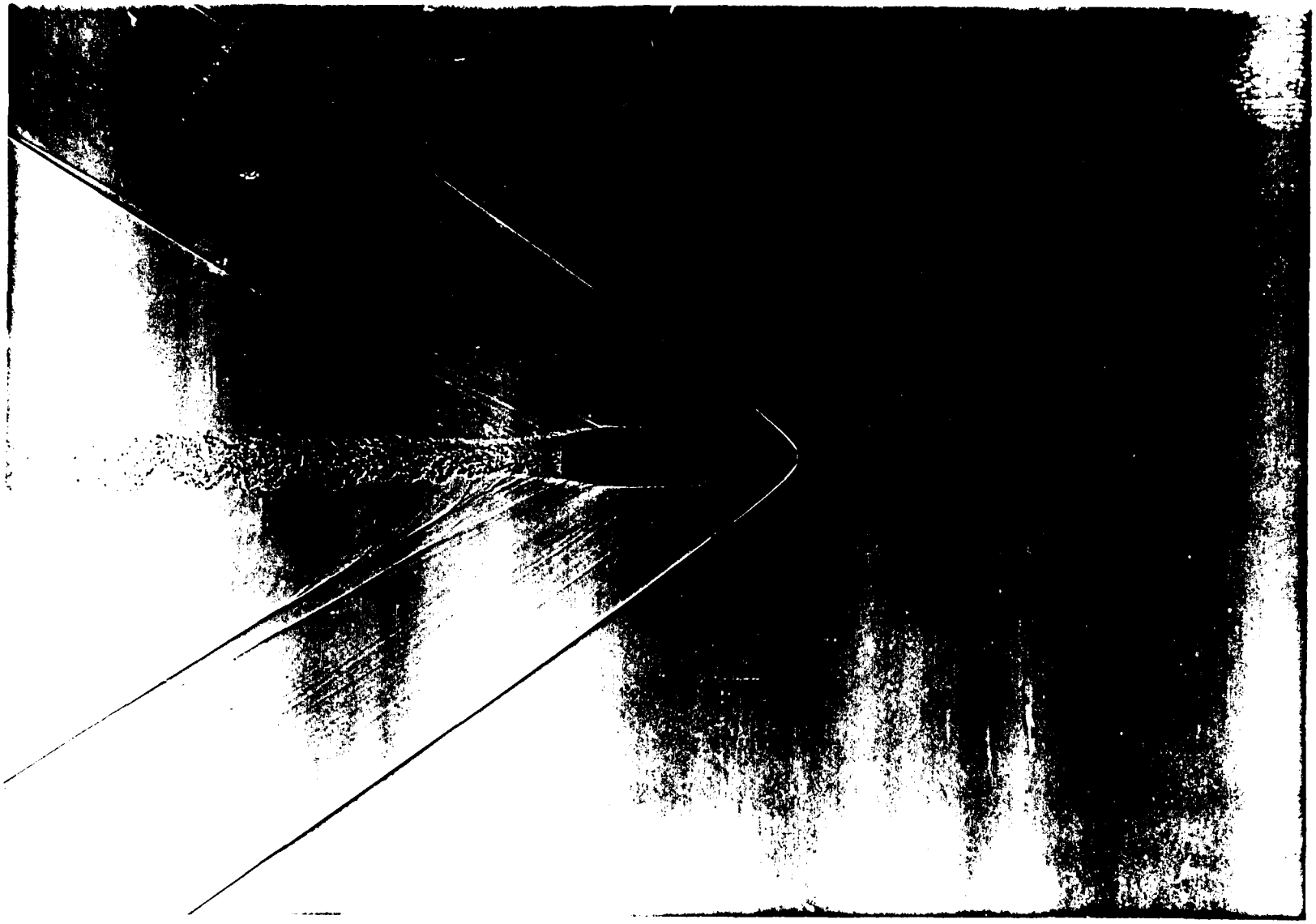

Figure 9. Shadowgraph of M118 Bullet at Mach 1.8.

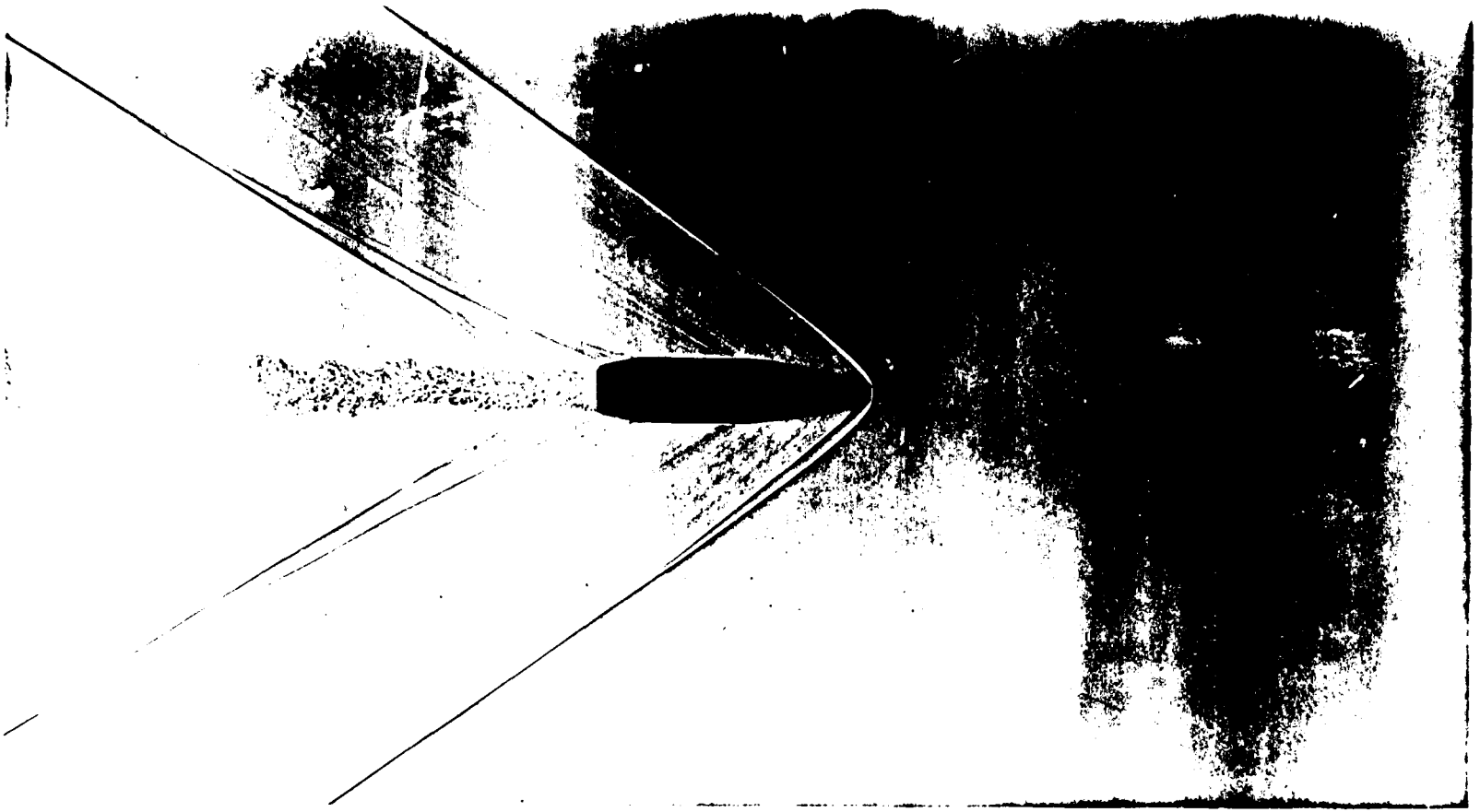

Figure 10. Shadowgraph of 190 Grain Sierra Bullet at Mach 1.8.

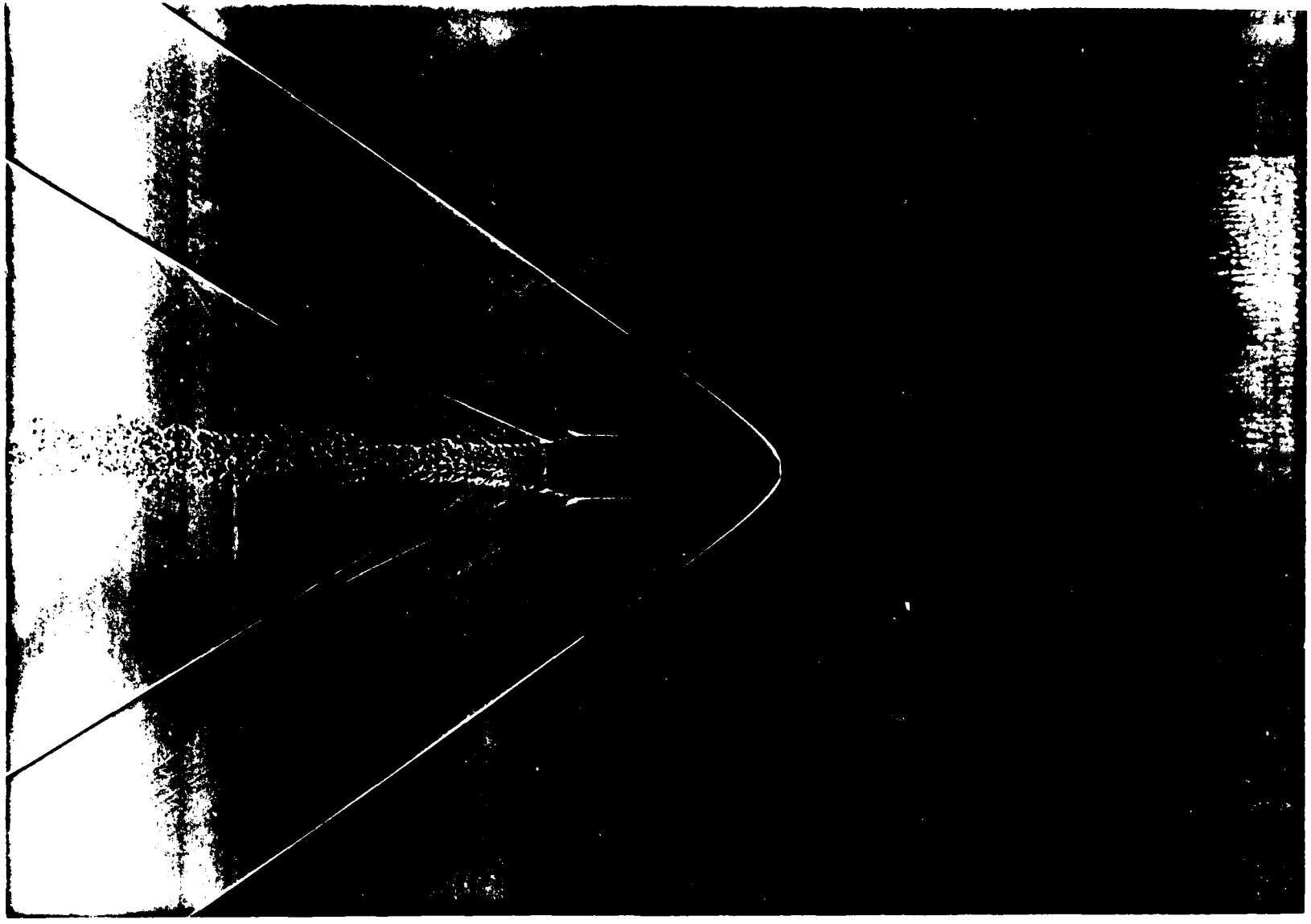

Figure 11. Shadowgraph of 168 Grain Sierra Bullet at Mach 1.8.

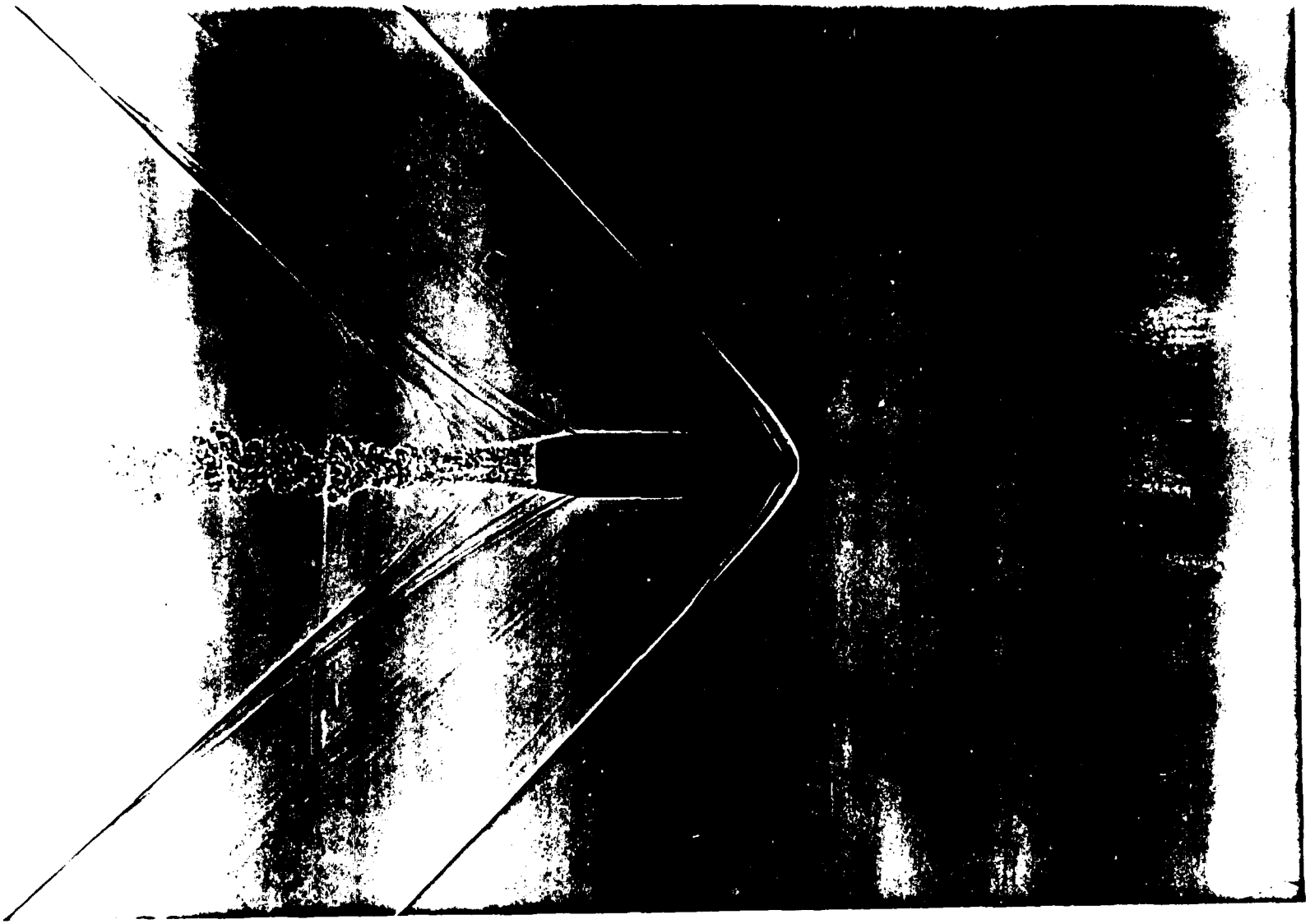

Figure 12. Shadowgraph of M118 Bullet at Mach 1.4.

Figure 13. Shadowgraph of 190 Grain Sierra Bullet at Mach 1.4.

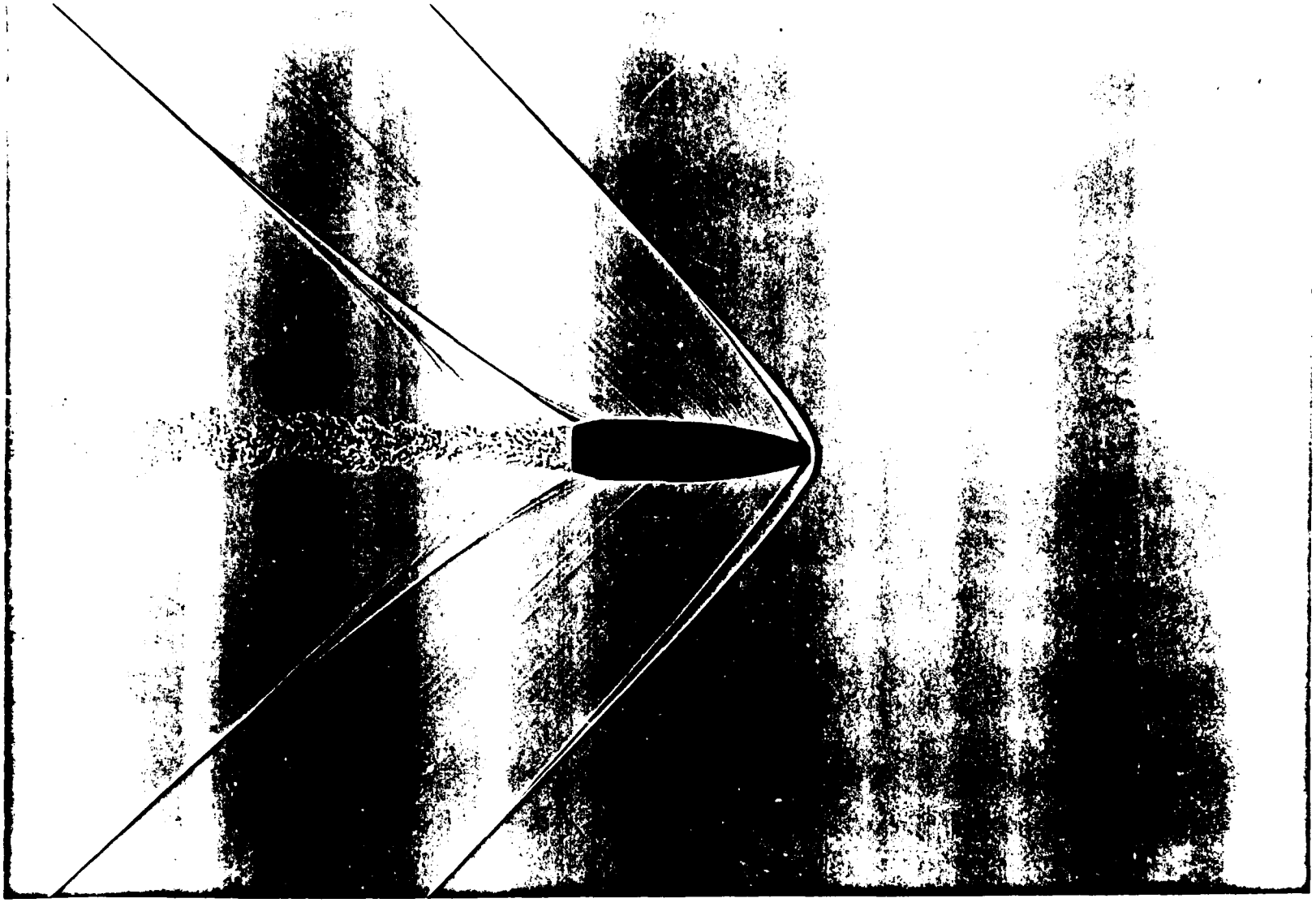

Figure 14. Shadowgraph of 168 Grain Sierra Bullet at Mach 1.4.

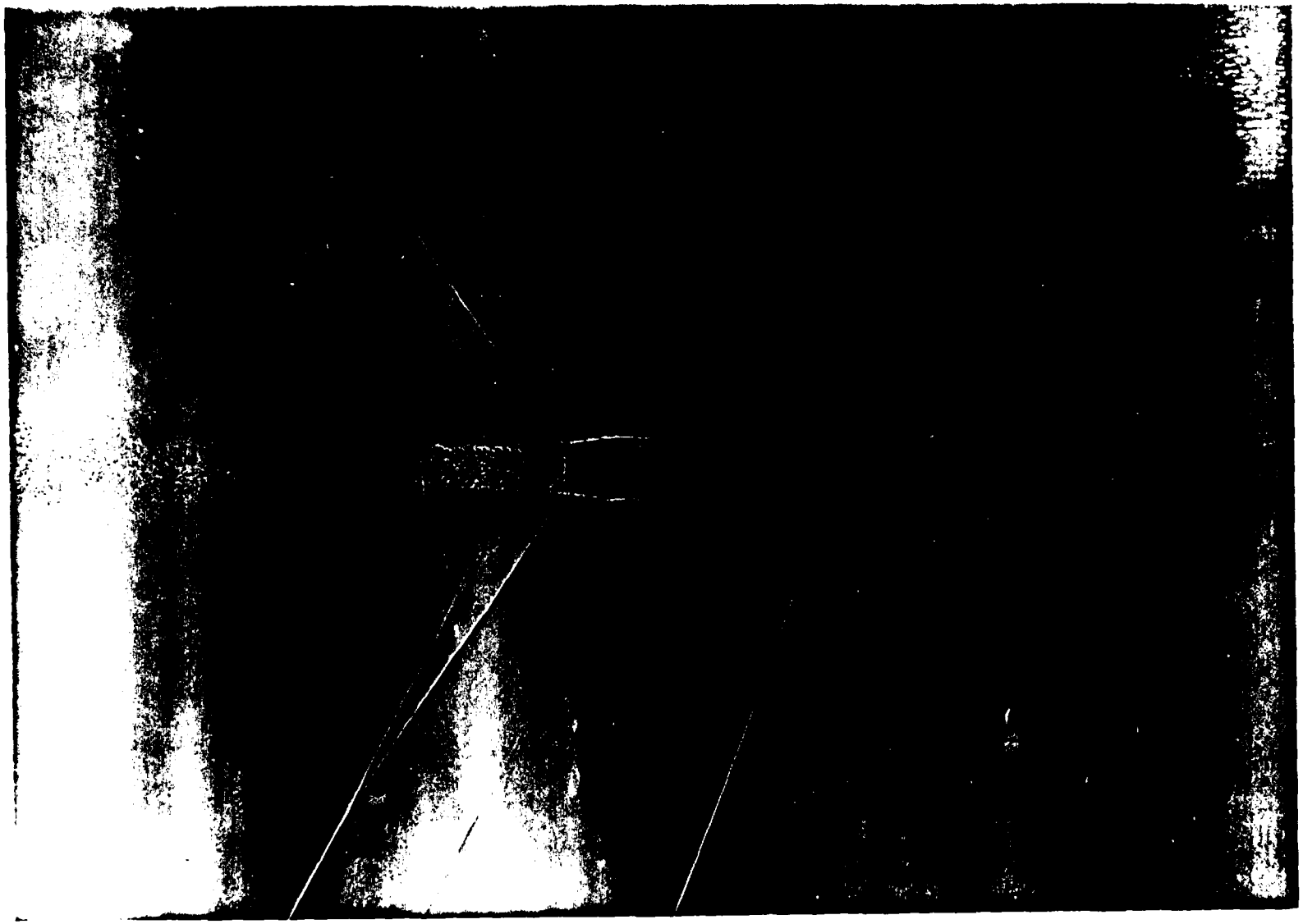

Figure 15. Shadowgraph of M118 Bullet at Mach 1.1.

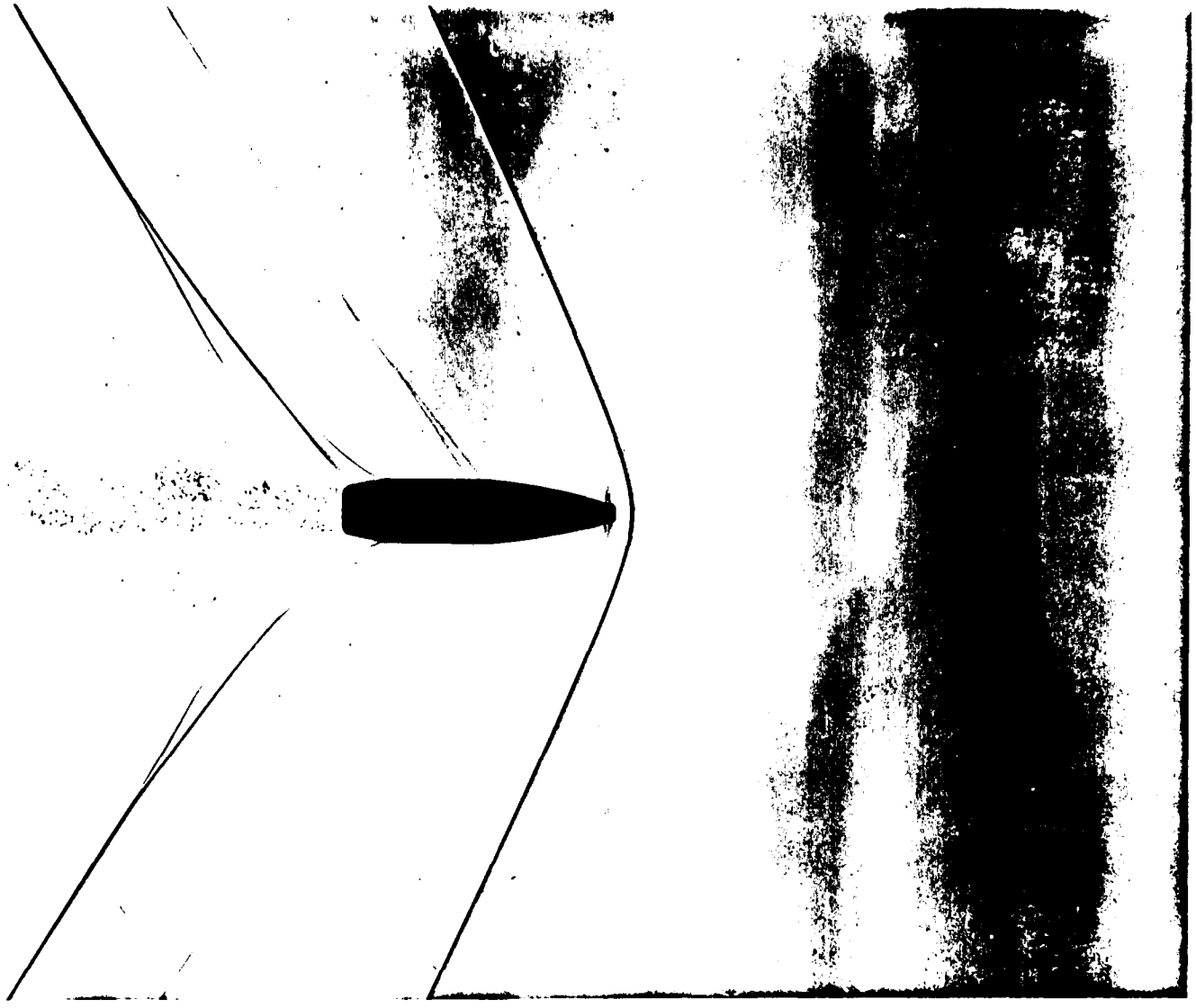

Figure 16. Shadowgraph of 190 Grain Sierra Bullet at Mach 1.1.

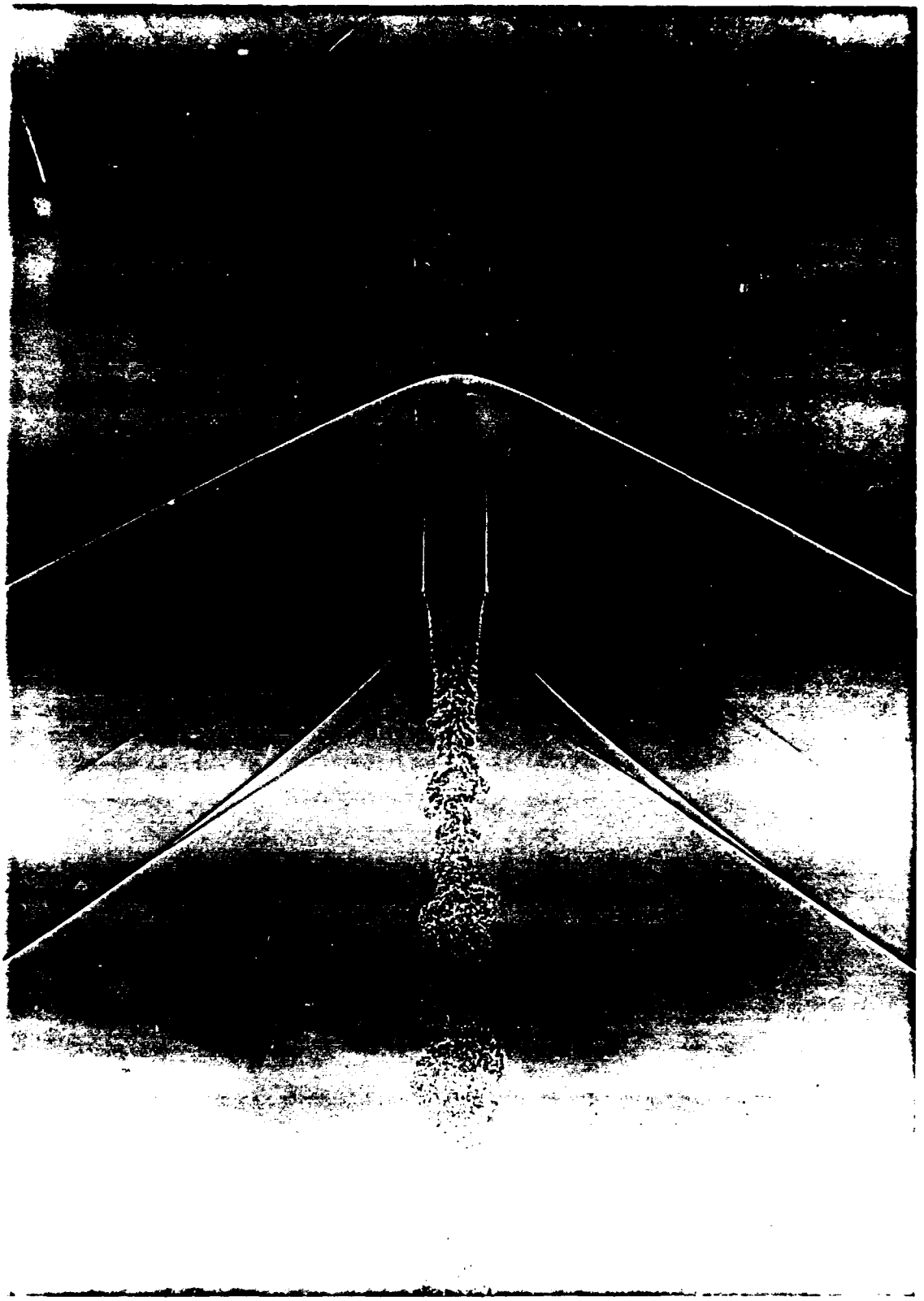

Figure 17. Shadowgraph of 168 Grain Sierra Bullet at Mach 1.1.

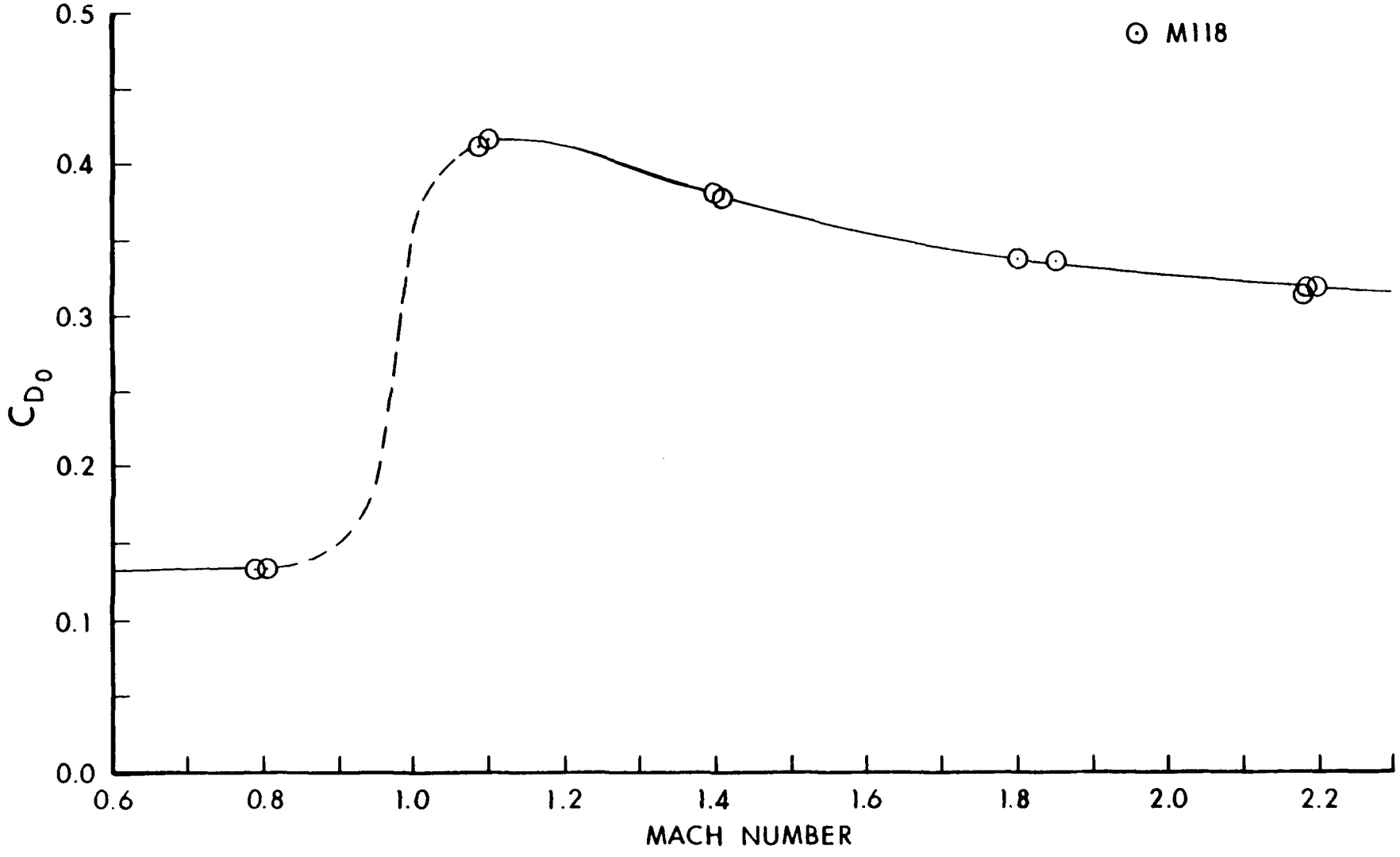

Figure 18. Zero-Yaw Drag Force Coefficient versus Mach Number, M118 Bullet.

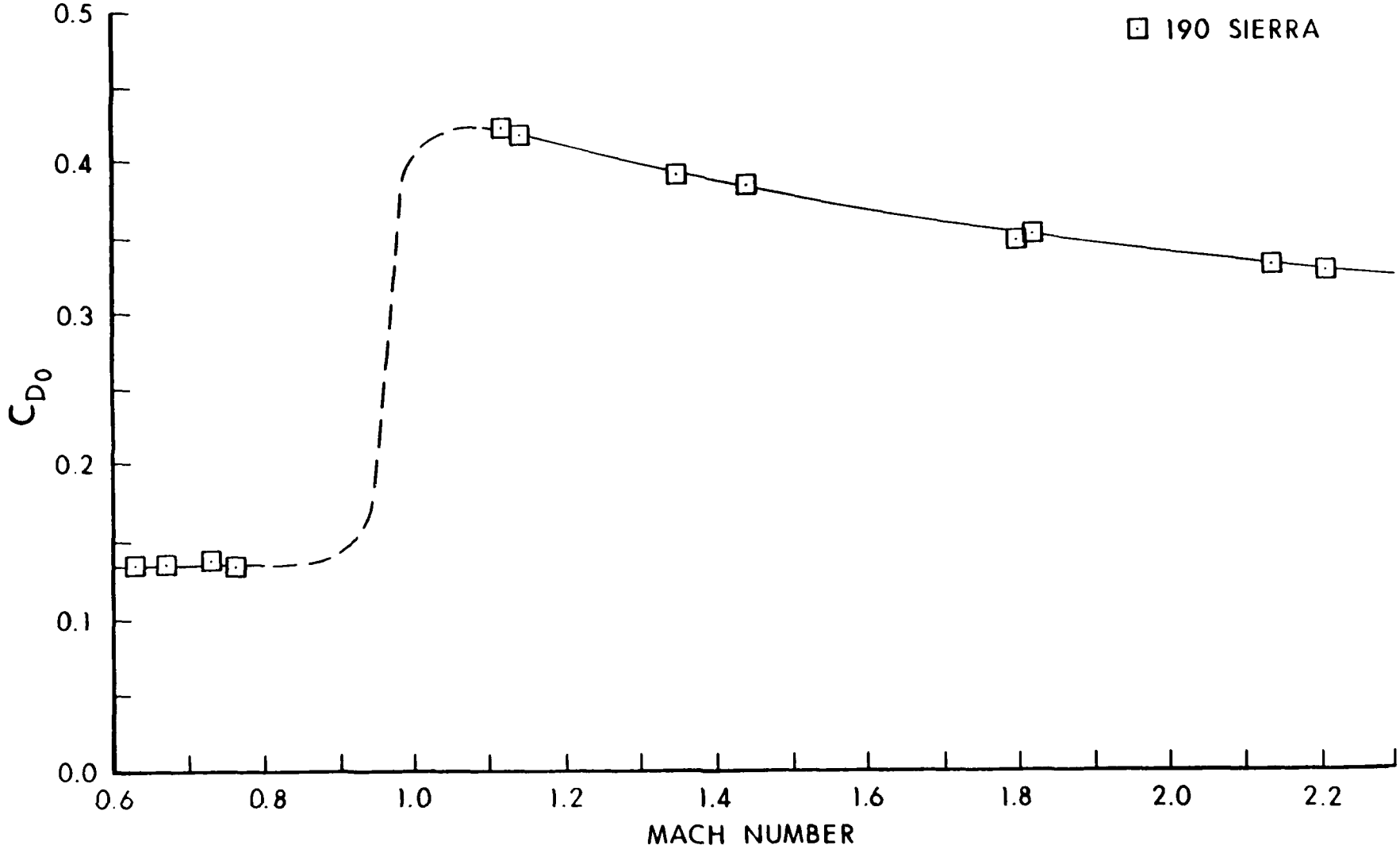

Figure 19. Zero-Yaw Drag Force Coefficient versus Mach Number, 190 Grain Sierra Bullet.

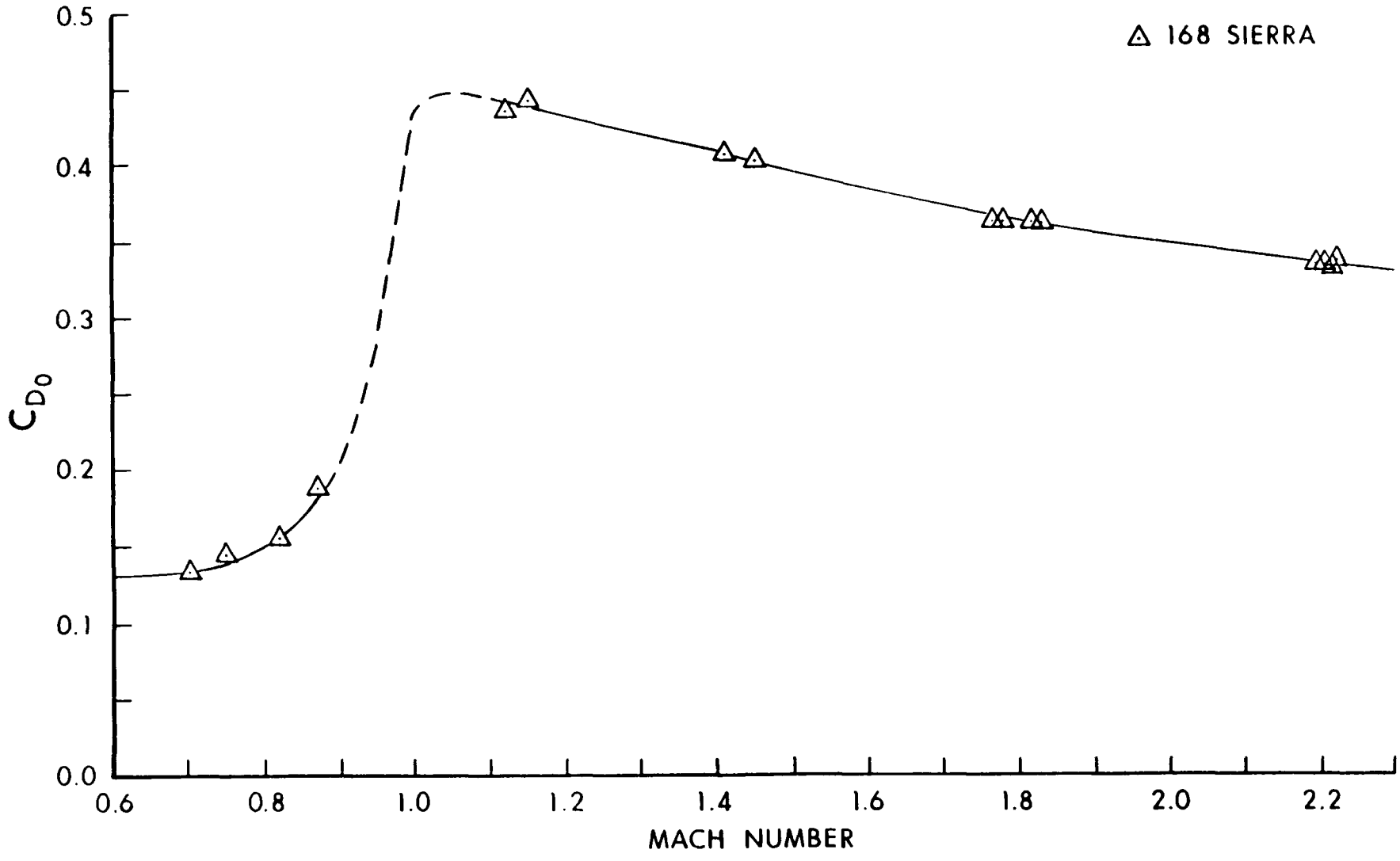

Figure 20. Zero-Yaw Drag Force Coefficient versus Mach Number, 168 Grain Sierra Bullet.

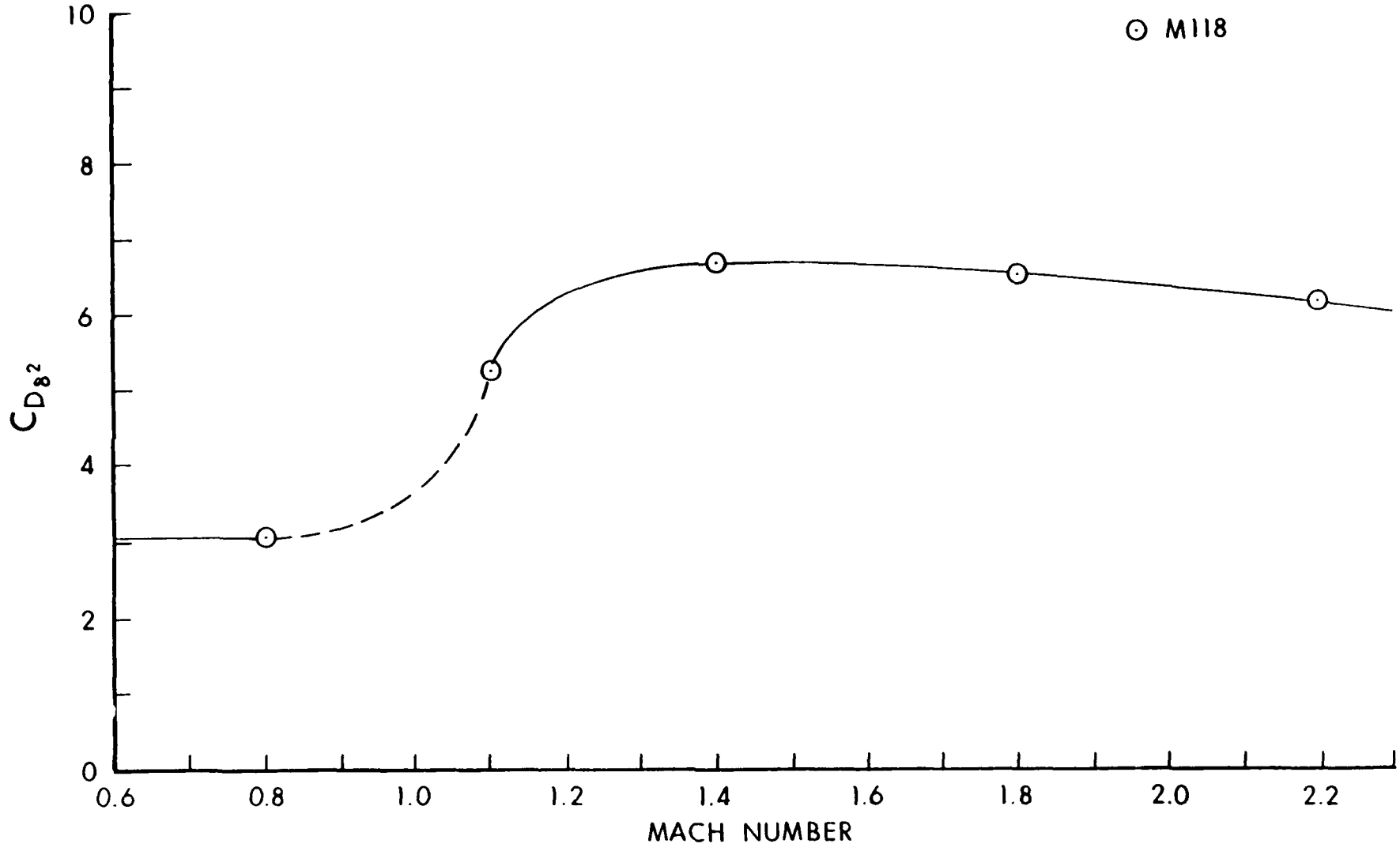

Figure 21. Yaw Drag Force Coefficient versus Mach Number, M118 Bullet.

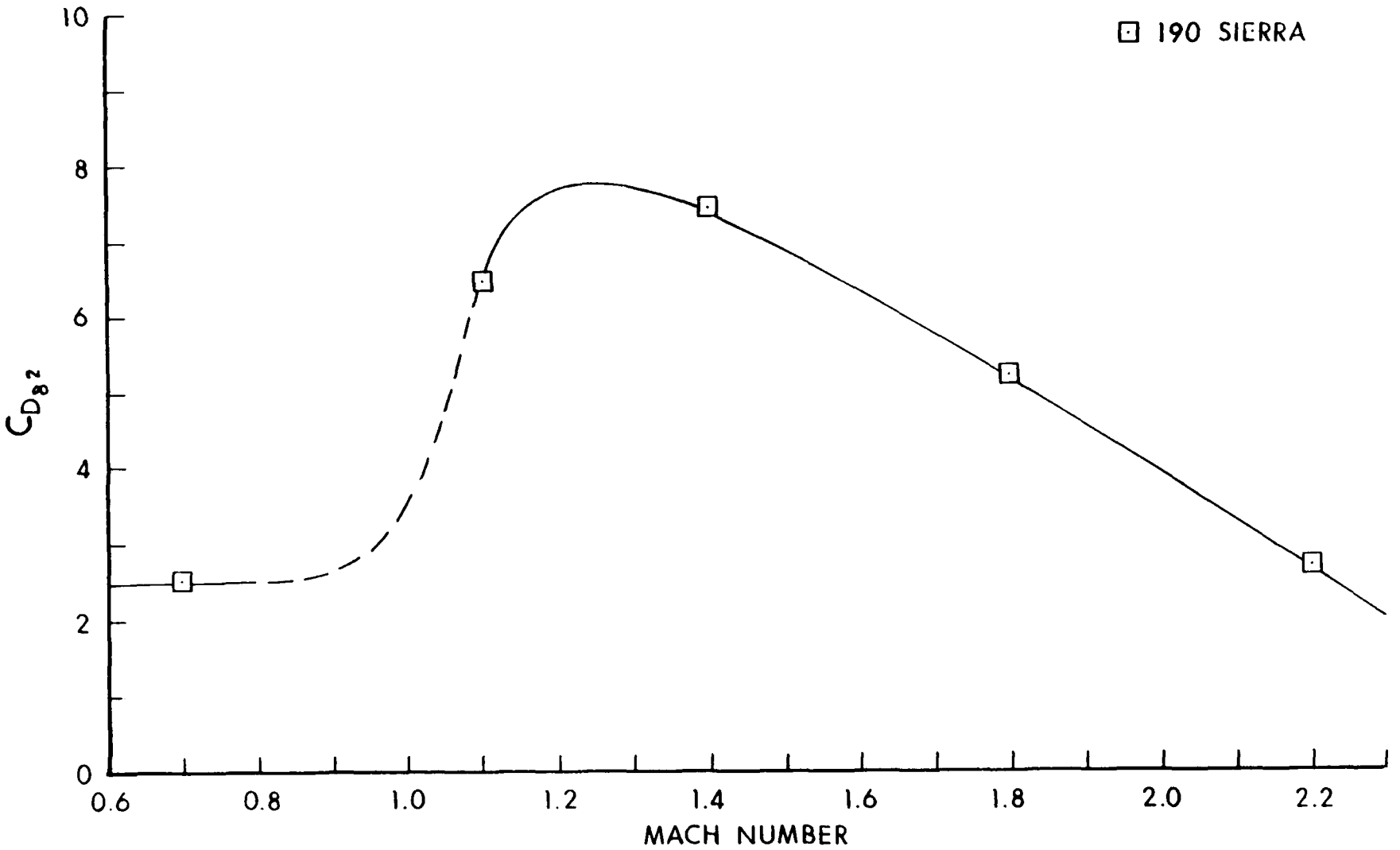

Figure 22. Yaw Drag Force Coefficient versus Mach Number, 190 Grain Sierra Bullet

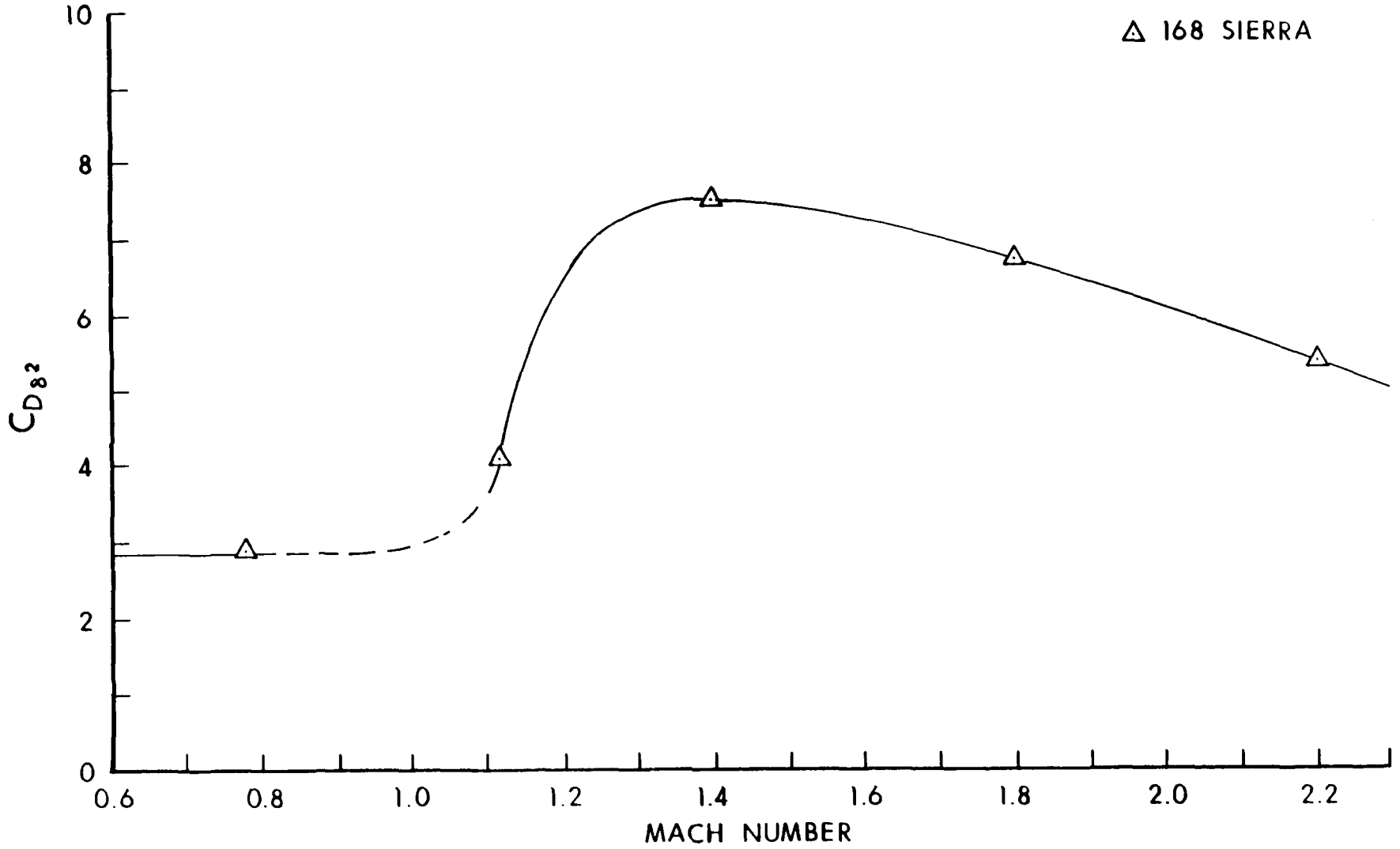

Figure 23. Yaw Drag Force Coefficient versus Mach Number, 168 Grain Sierra Bullet

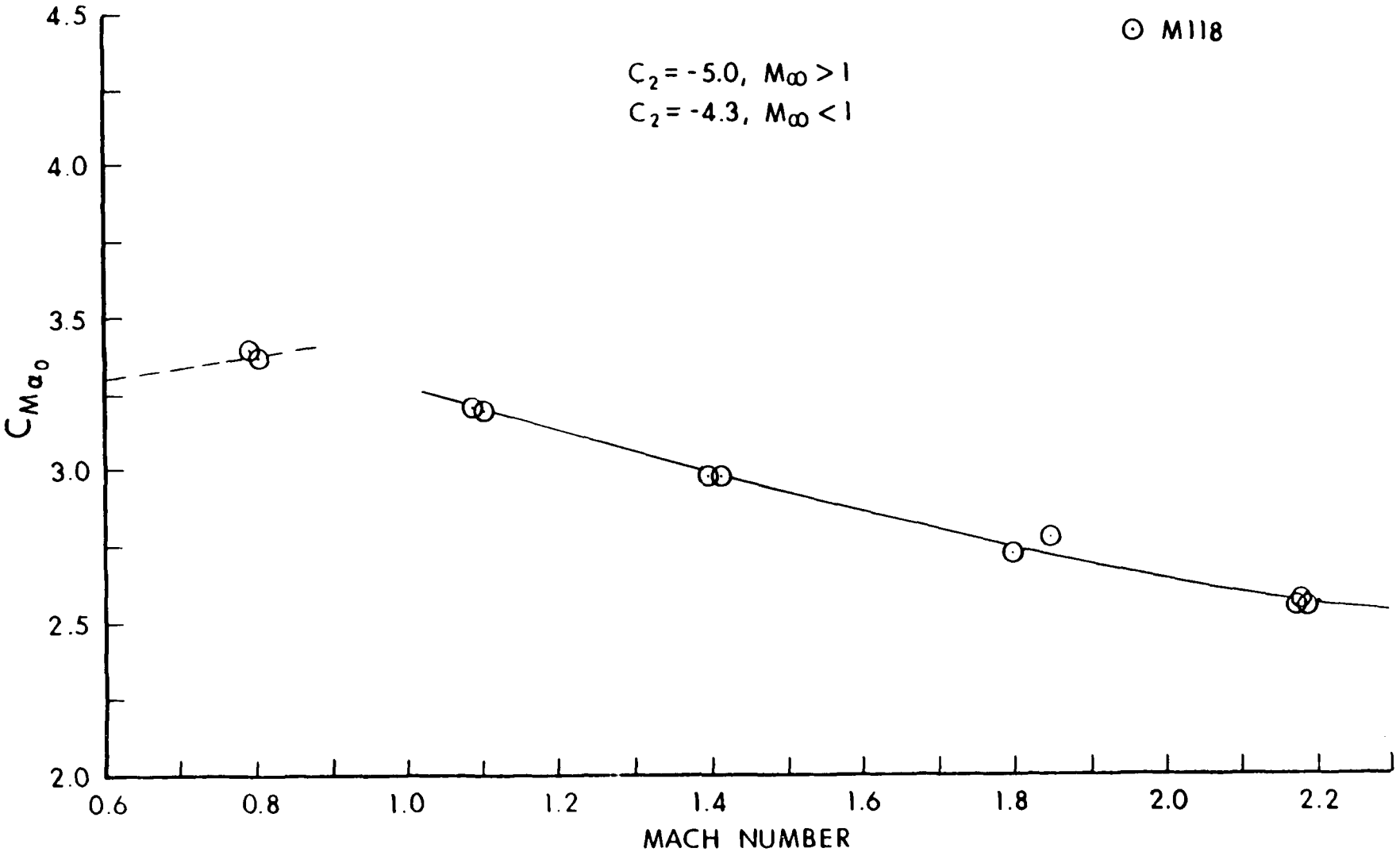

Figure 24. Zero-Yaw Overturning Moment Coefficient versus Mach Number, M118 Bullet.

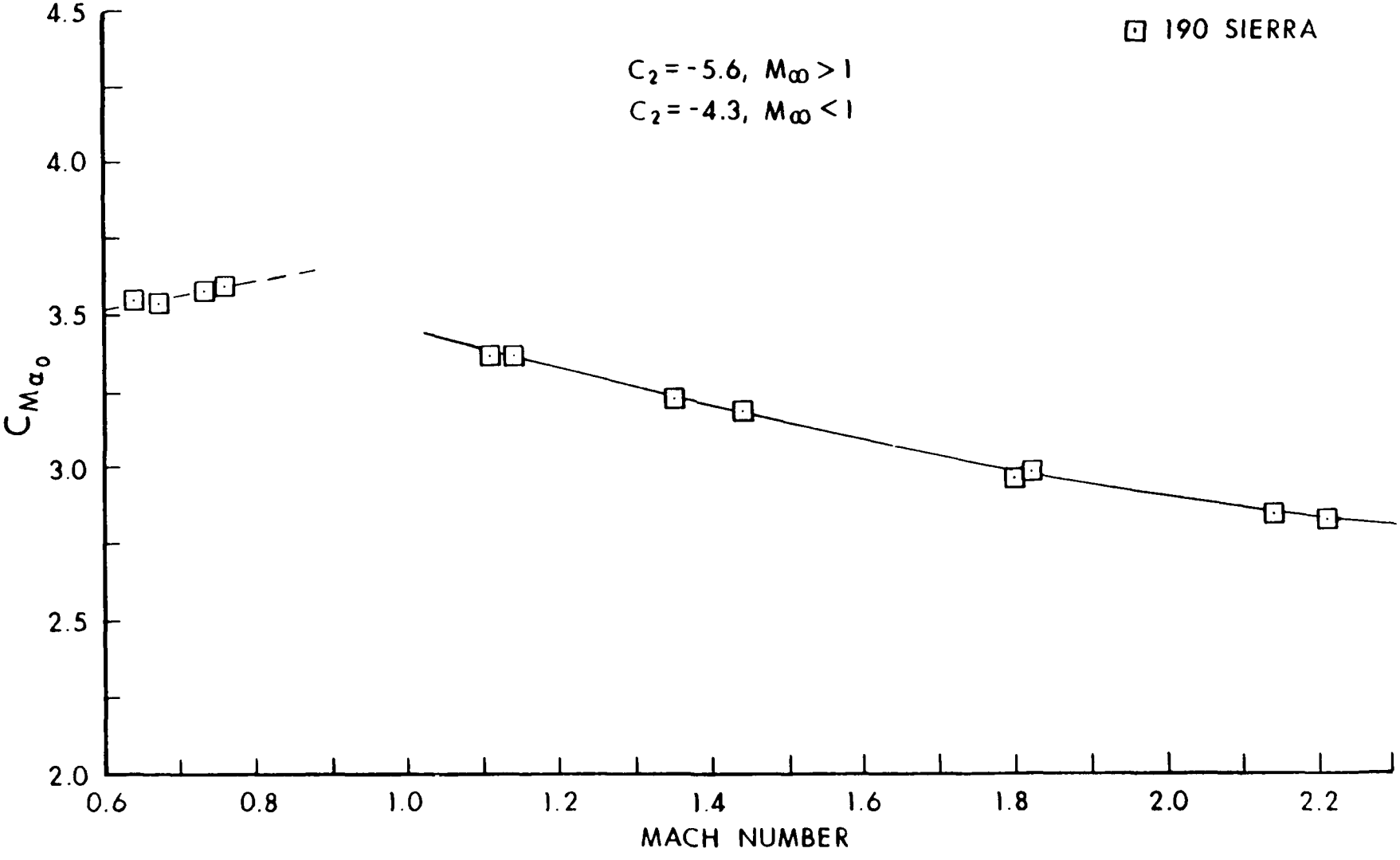

Figure 25. Zero-Yaw Overturning Moment Coefficient versus Mach Number, 190 Grain Sierra Bullet.

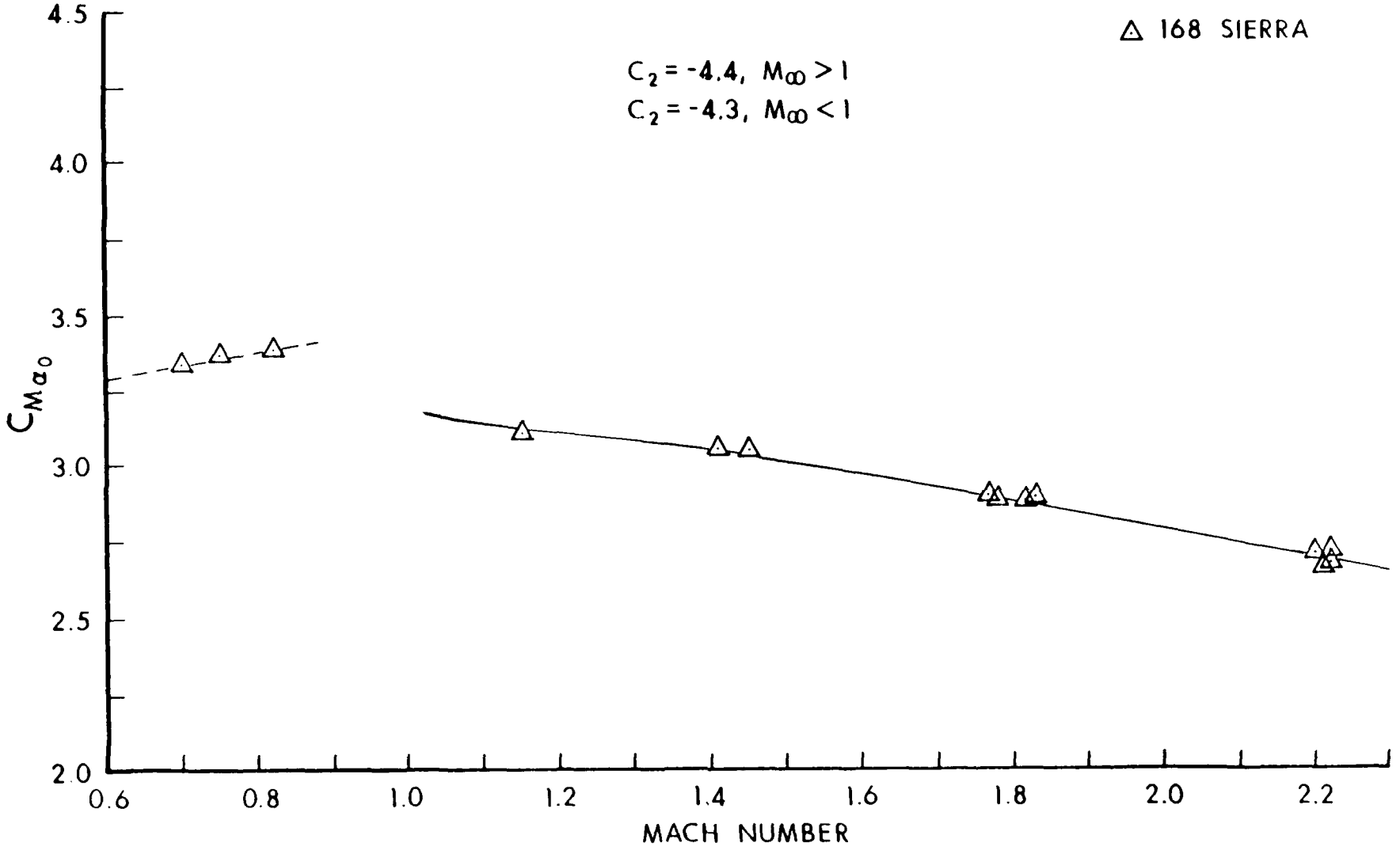

Figure 26. Zero-Yaw Overturning Moment Coefficient versus Mach Number, 168 Grain Sierra Bullet.

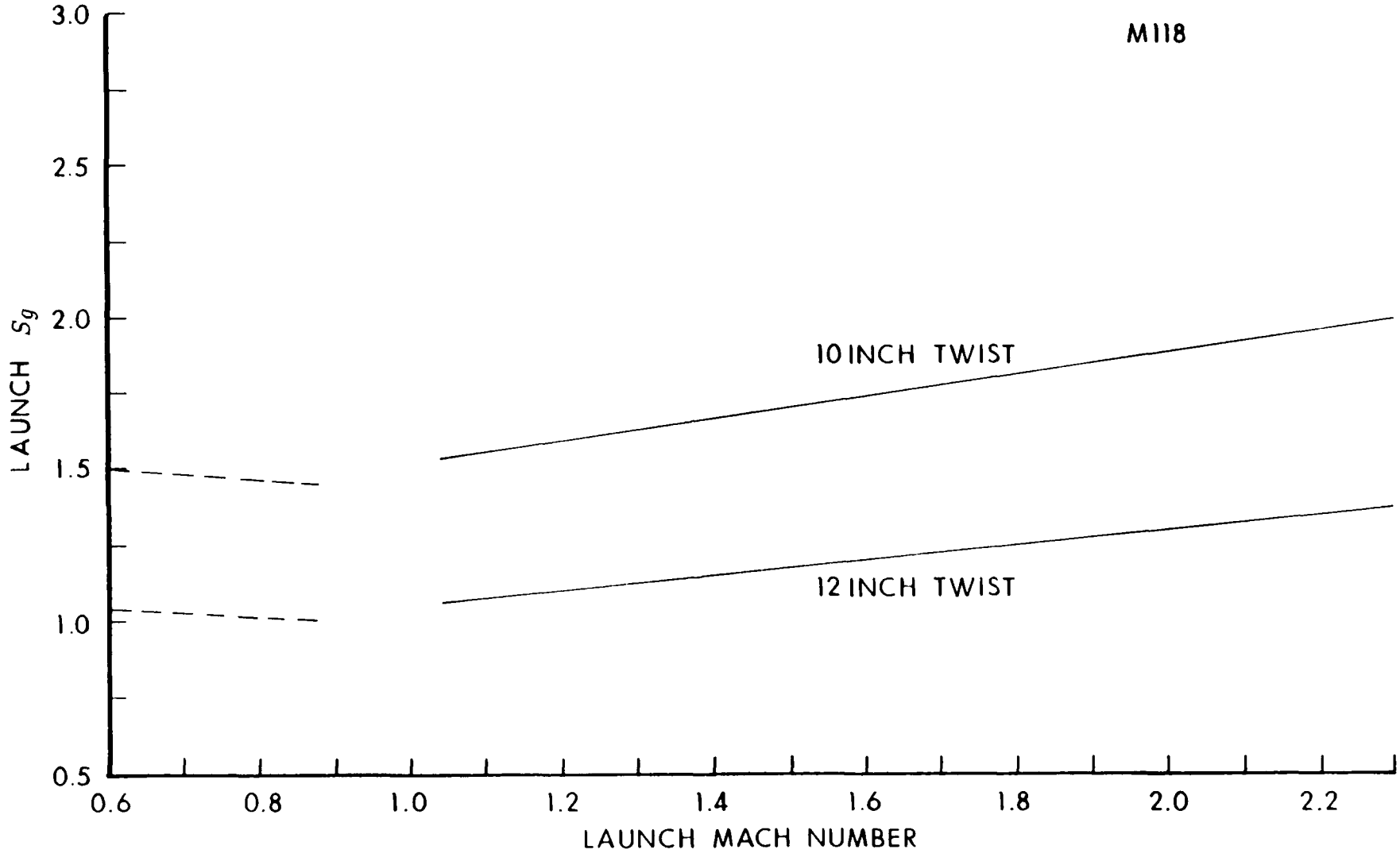

Figure 27. Gyroscopic Stability Factor versus Mach Number, M118 Bullet.

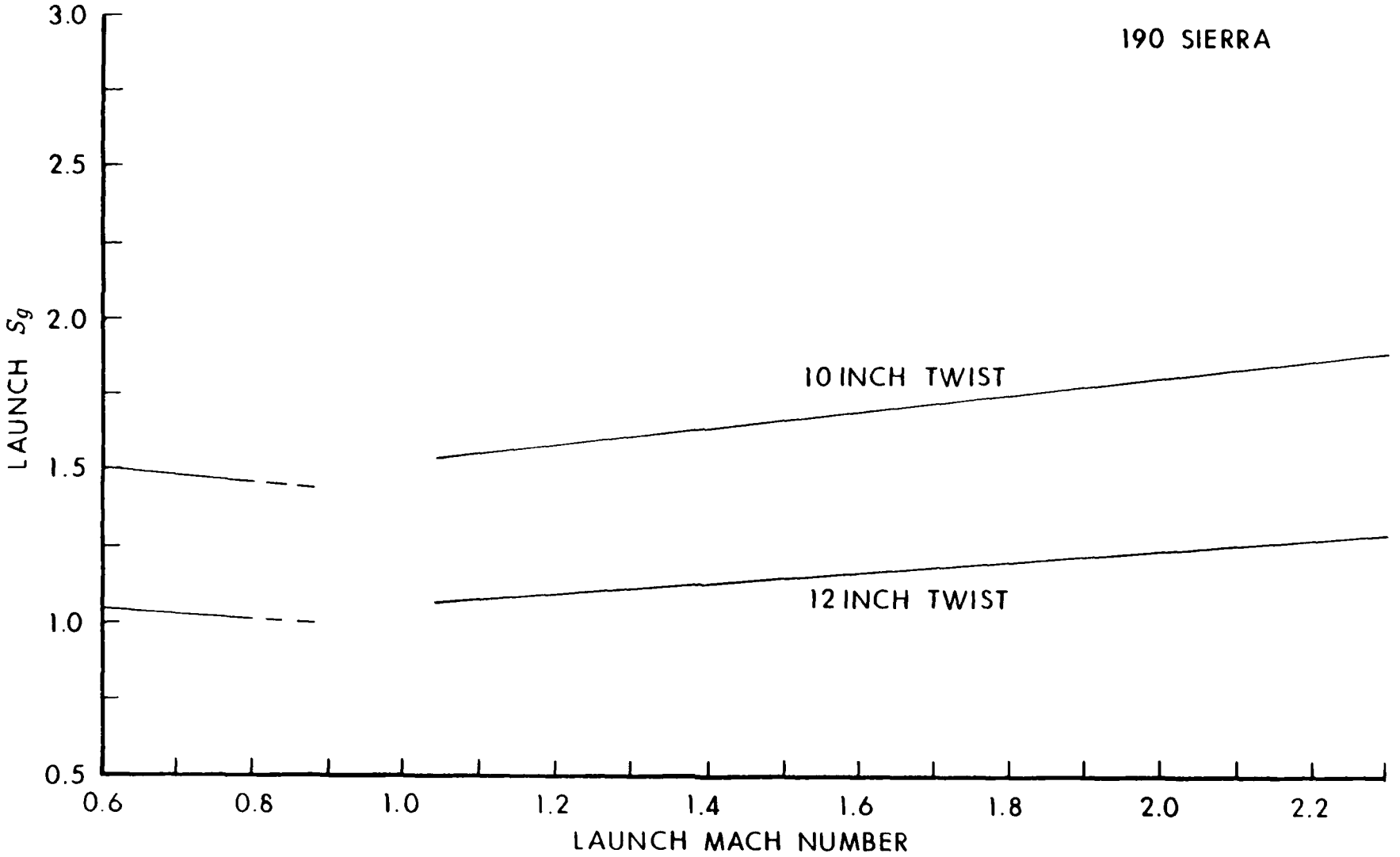

Figure 28. Gyroscopic Stability Factor versus Mach Number, 190 Grain Sierra Bullet

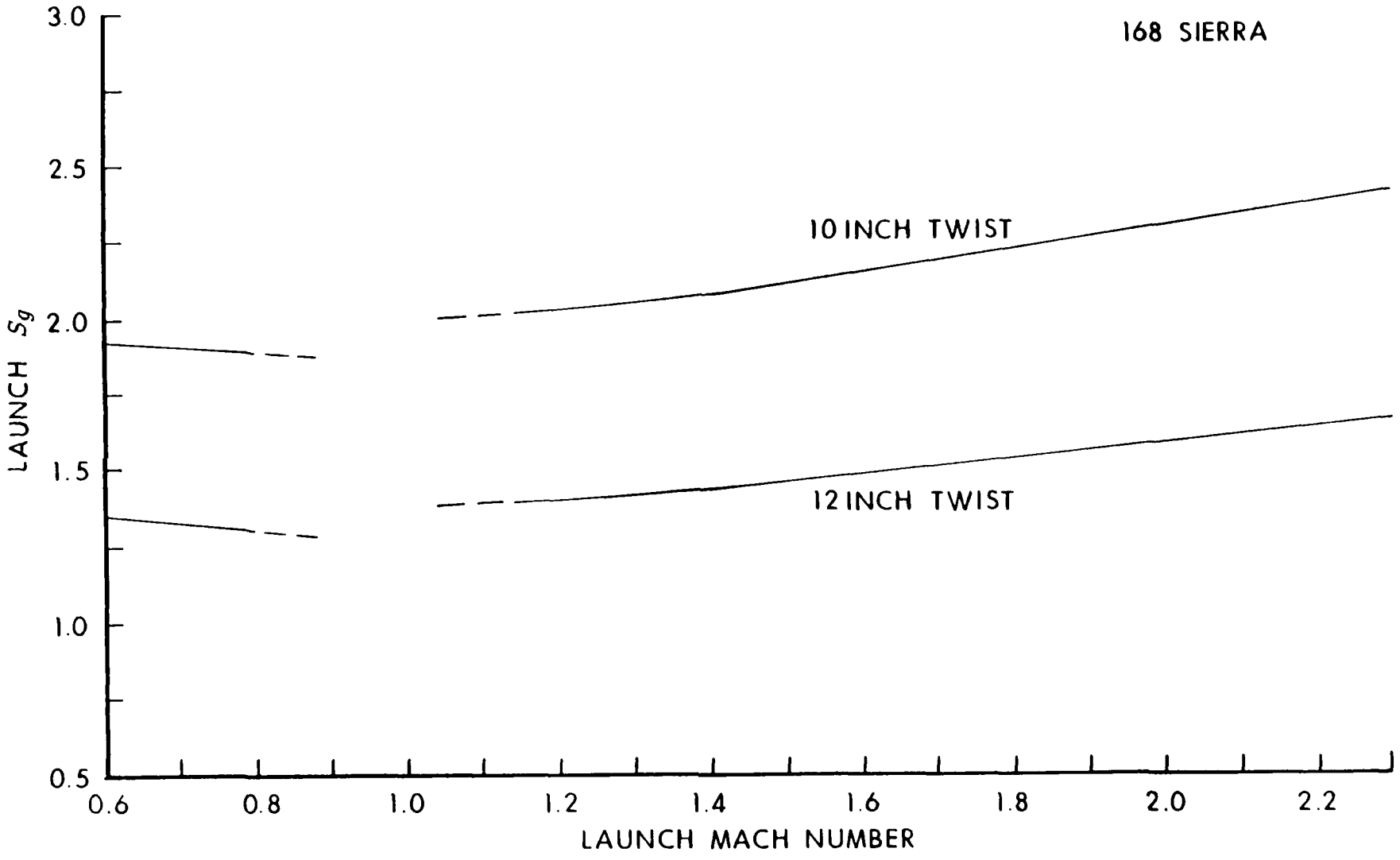

Figure 29. Gyroscopic Stability Factor versus Mach Number, 168 Grain Sierra Bullet

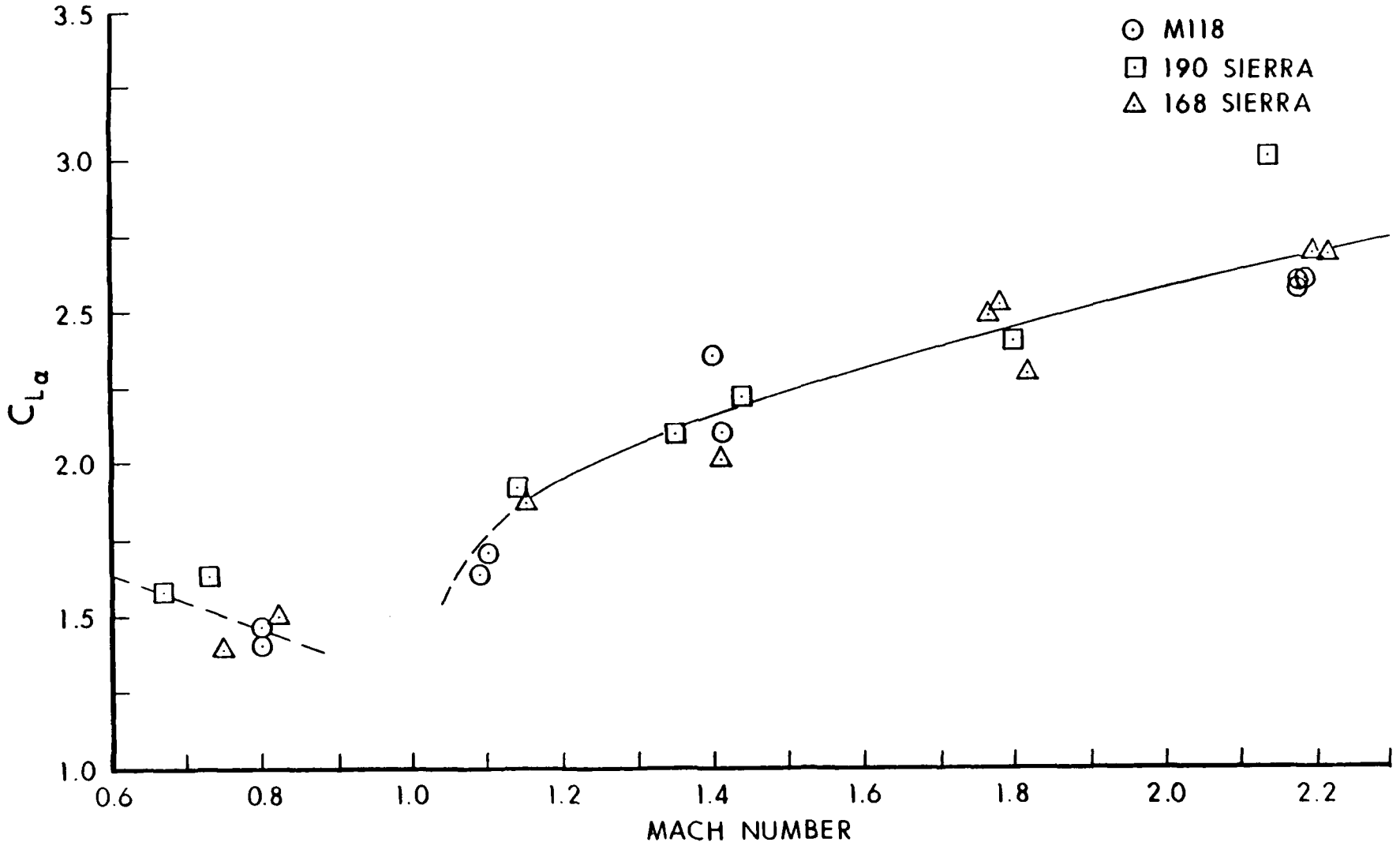

Figure 30. Lift Force Coefficient versus Mach Number.

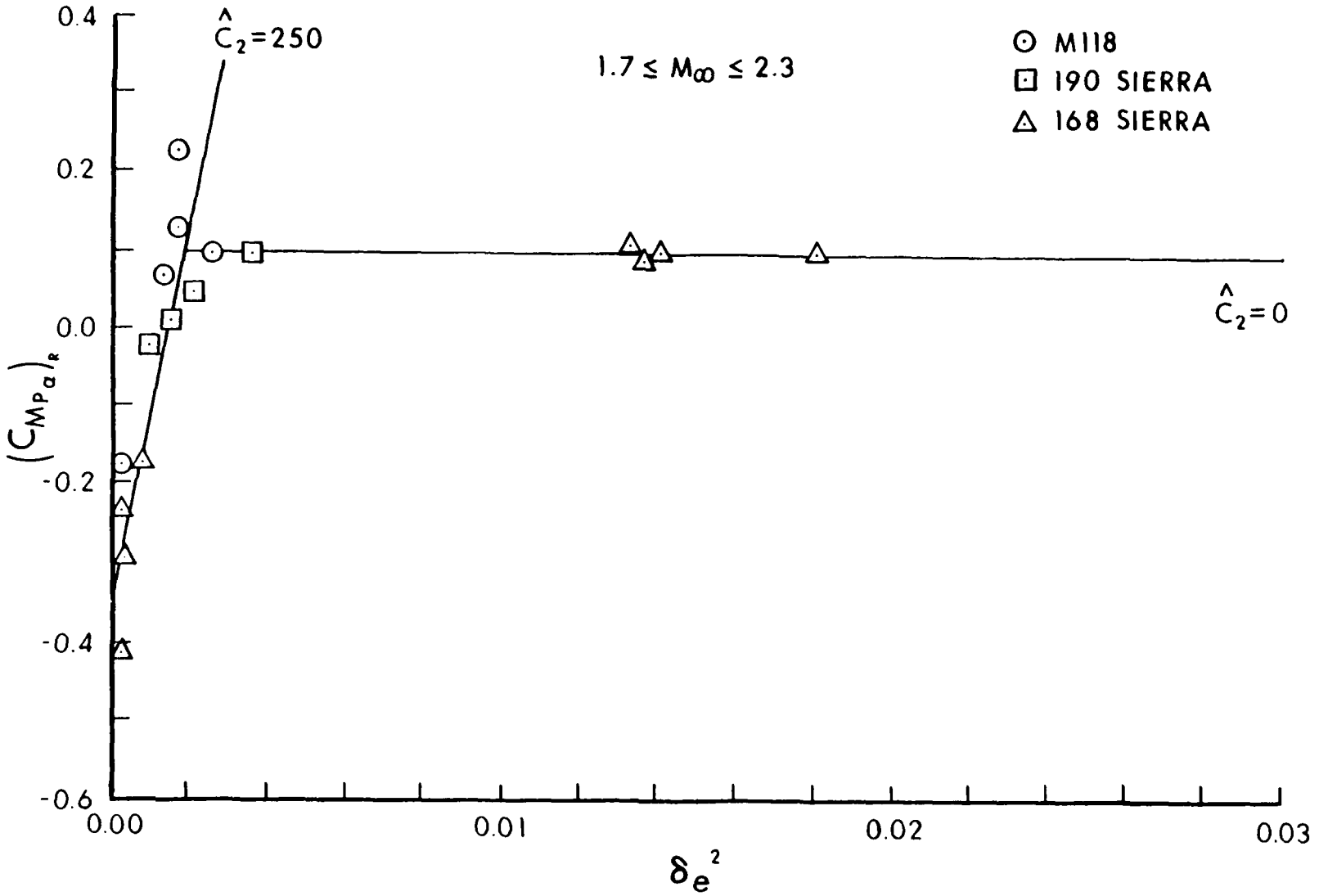

Figure 31. Magnus Moment Coefficient versus Effective Squared Yaw.

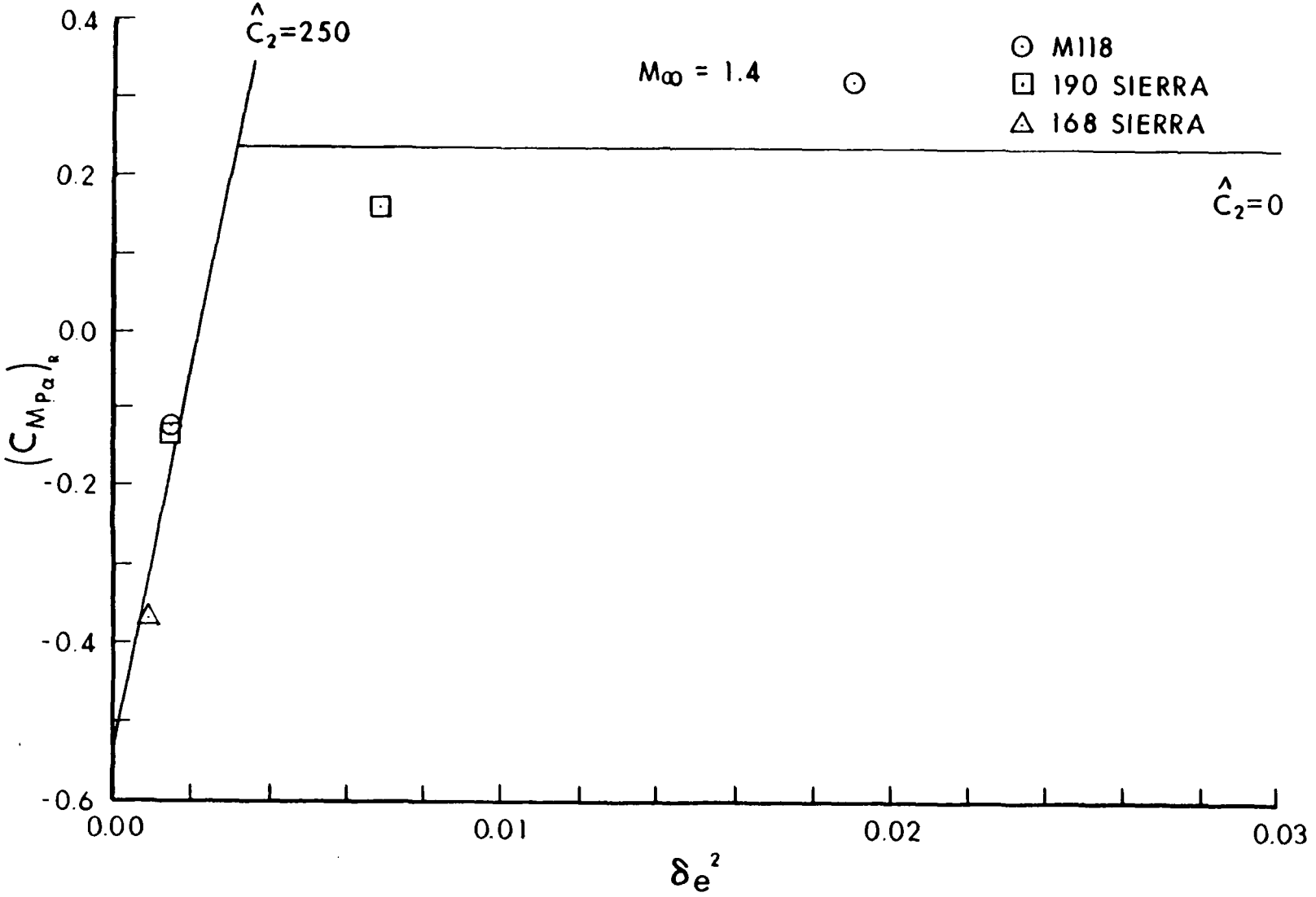

Figure 32. Magnus Moment Coefficient versus Effective Squared Yaw.

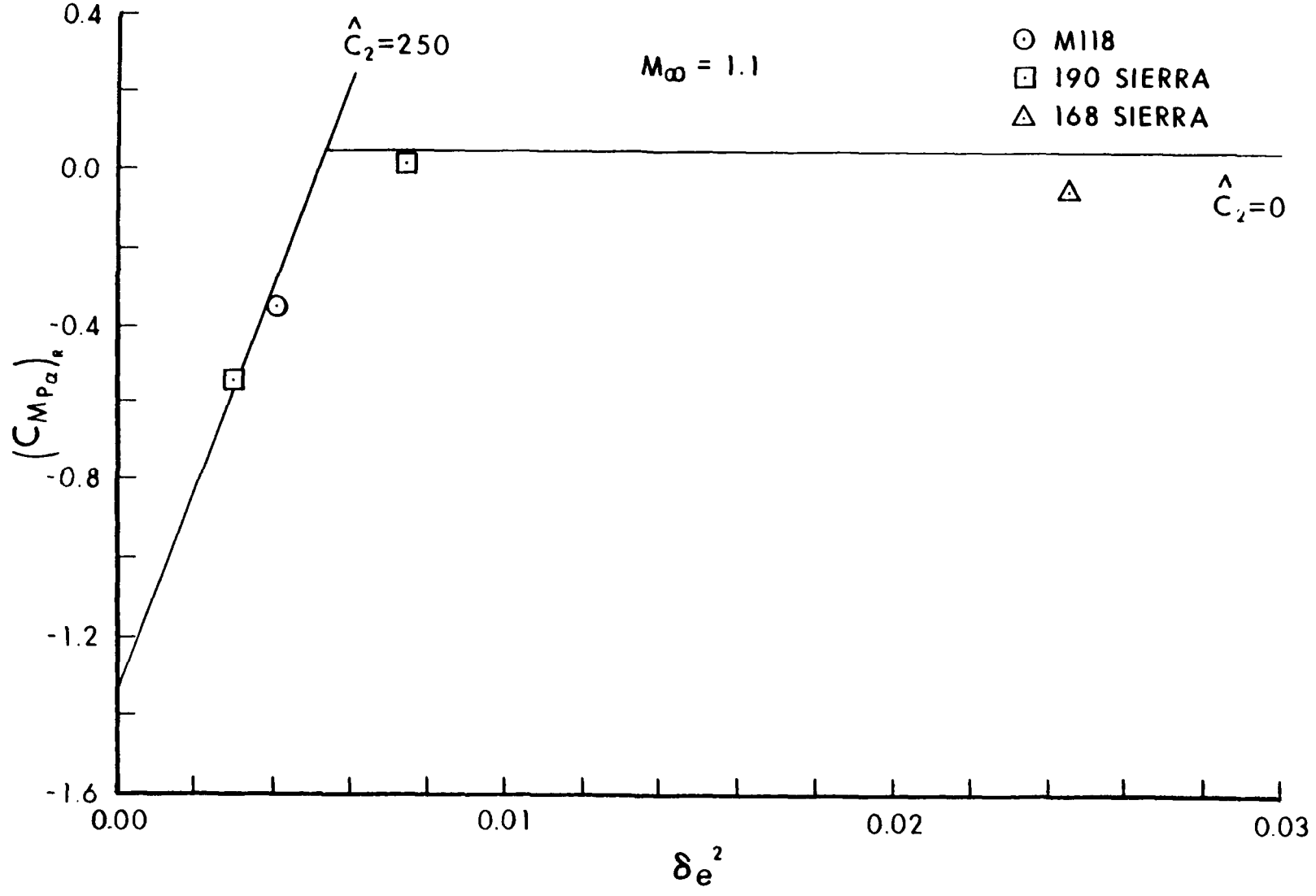

Figure 33. Magnus Moment Coefficient versus Effective Squared Yaw.

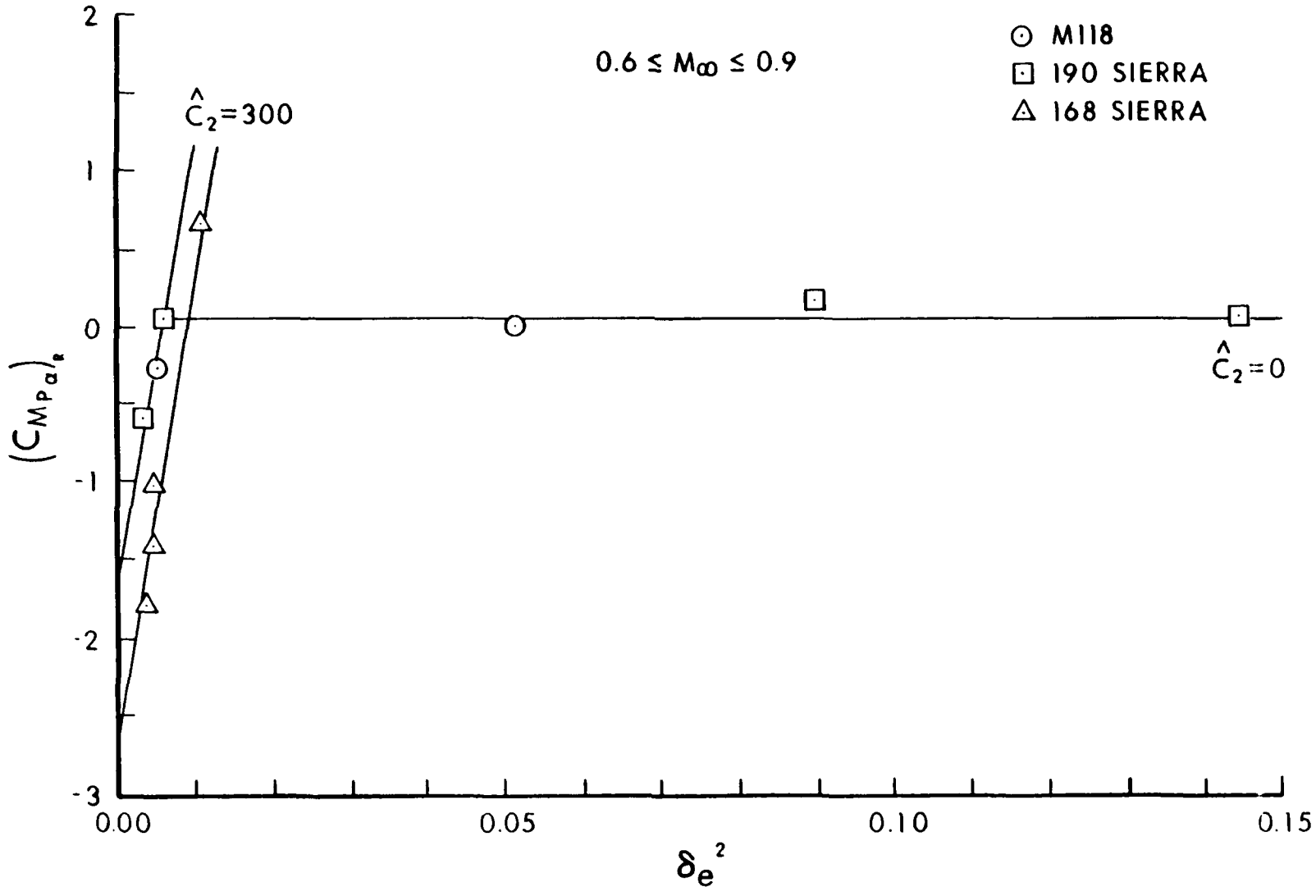

Figure 34. Magnus Moment Coefficient versus Effective Squared Yaw.

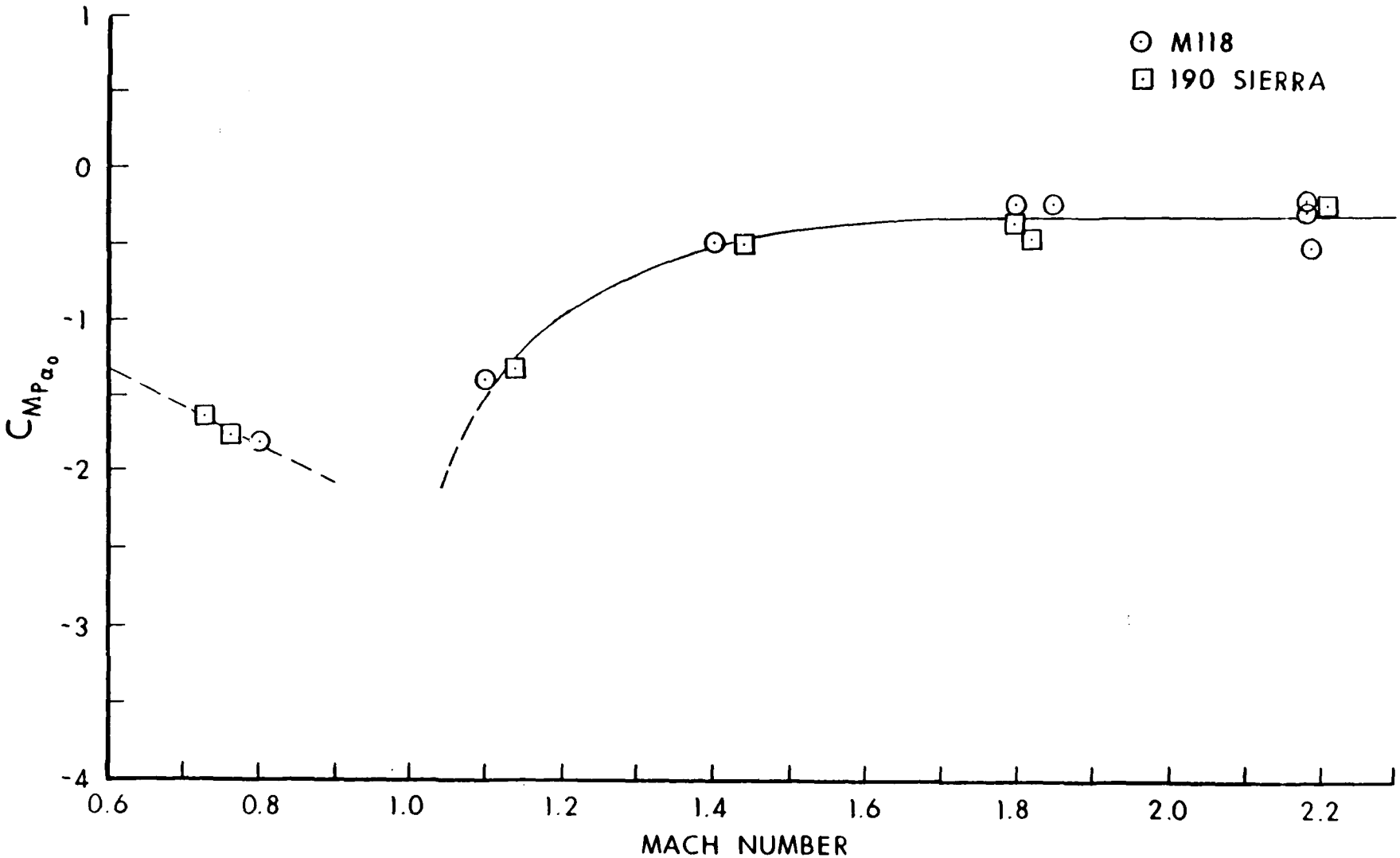

Figure 35. Zero Yaw Magnus Moment Coefficient versus Mach Number.

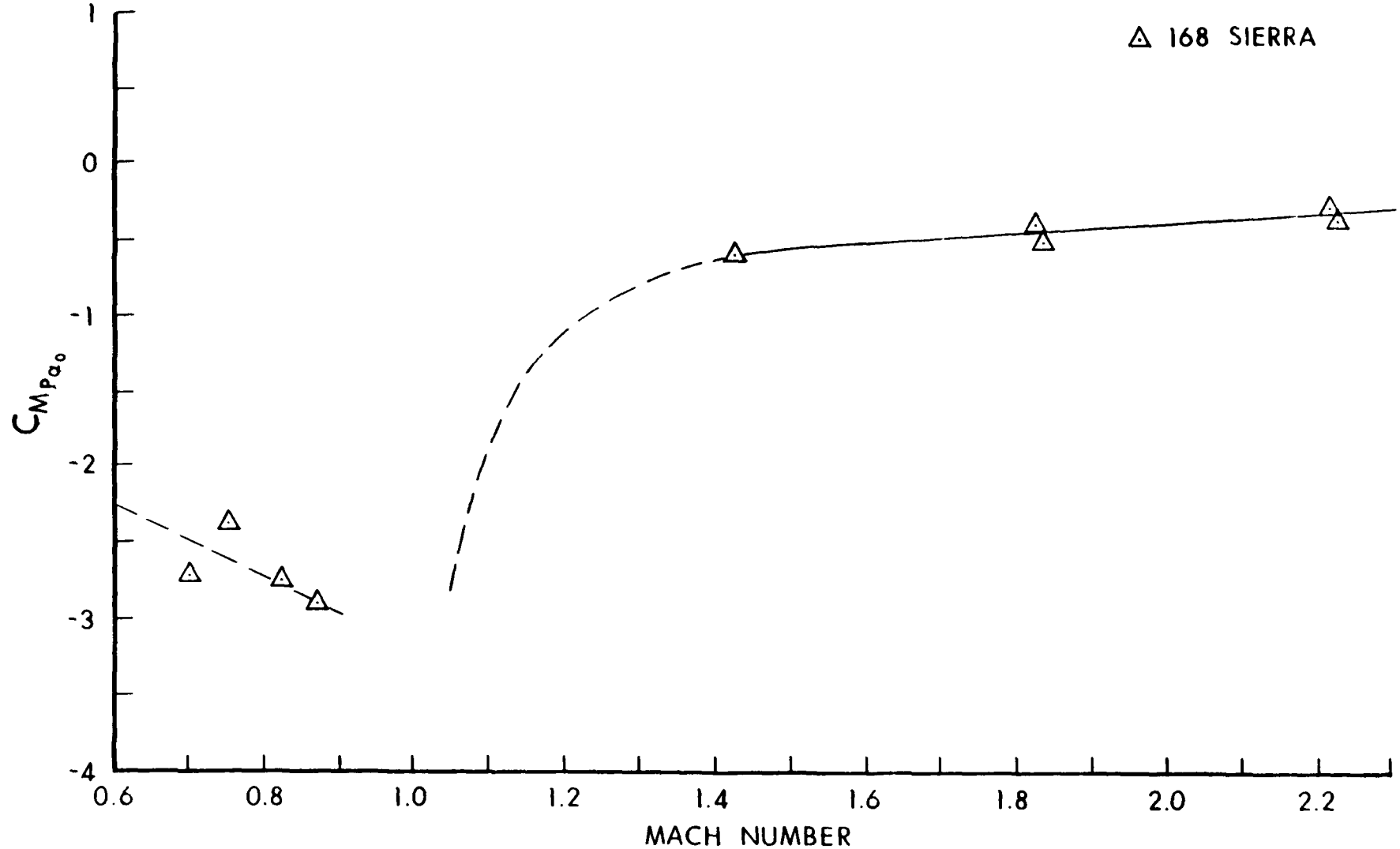

Figure 36. Zero-Yaw Magnus Moment Coefficient versus Mach Number.

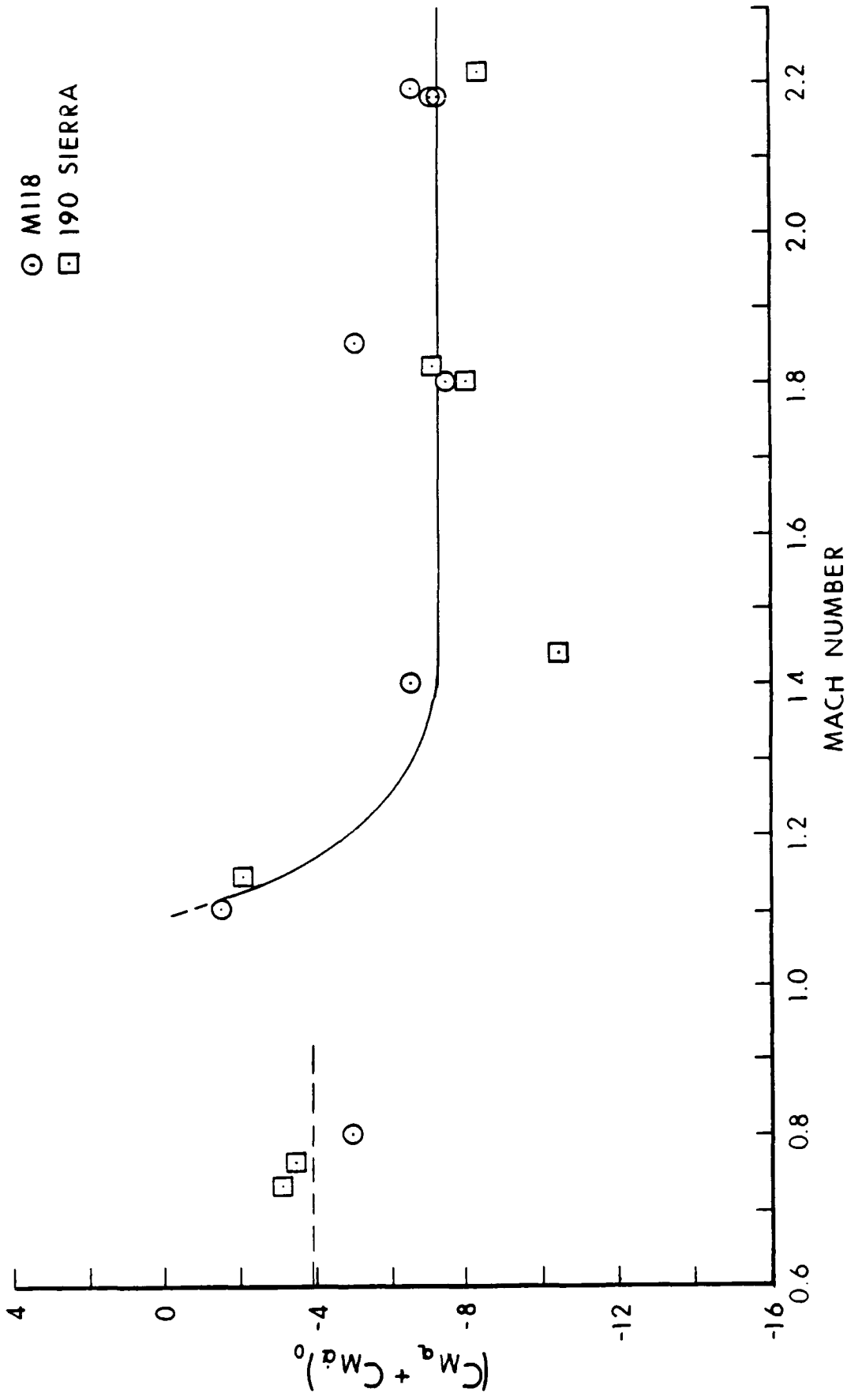

Figure 37. Zero-Yaw Pitch Damping Moment Coefficient versus Mach Number.

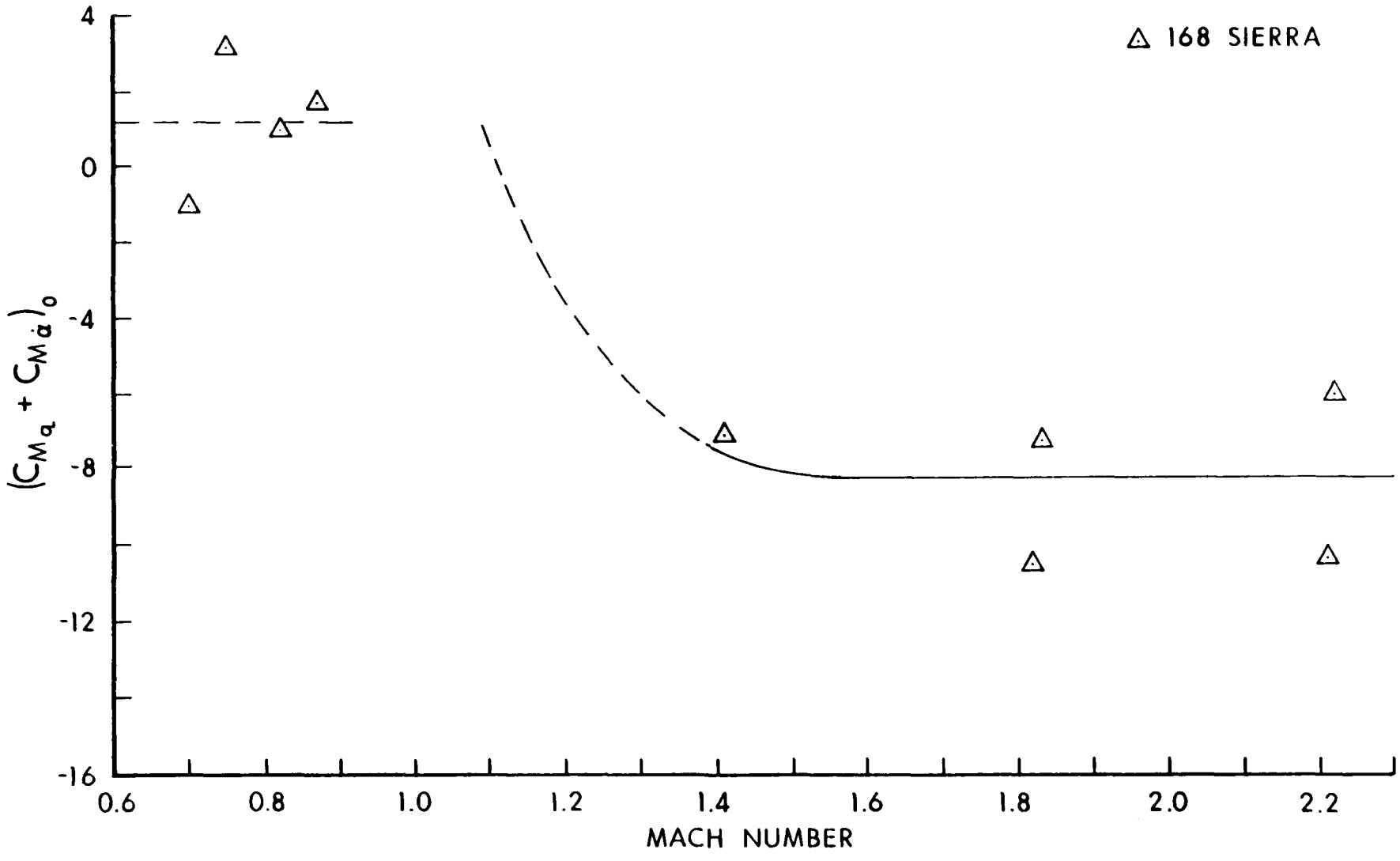

Figure 38. Zero Yaw Pitch Damping Moment Coefficient versus Mach Number.

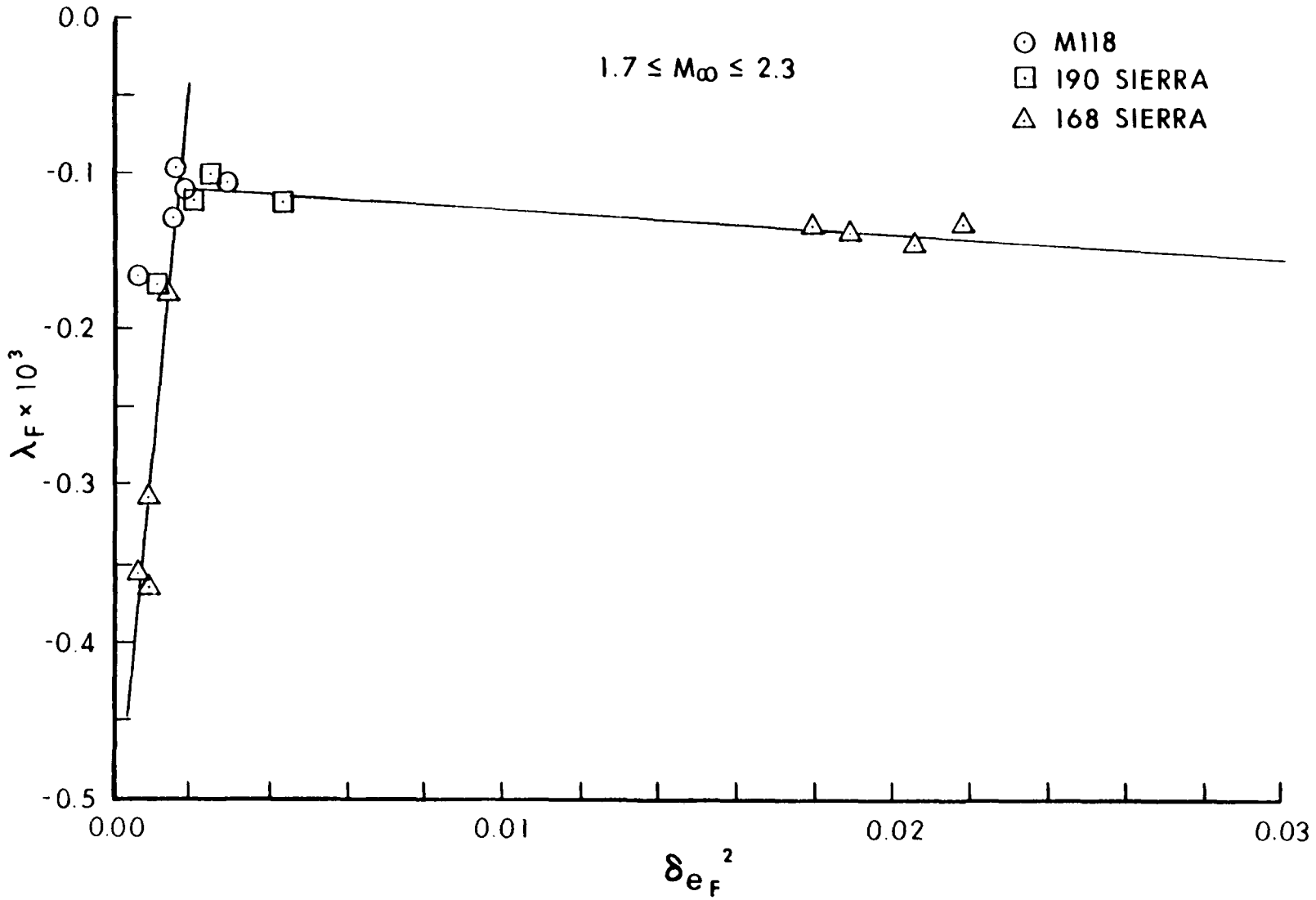

Figure 39. Fast Arm Damping Rate versus Effective Squared Yaw.

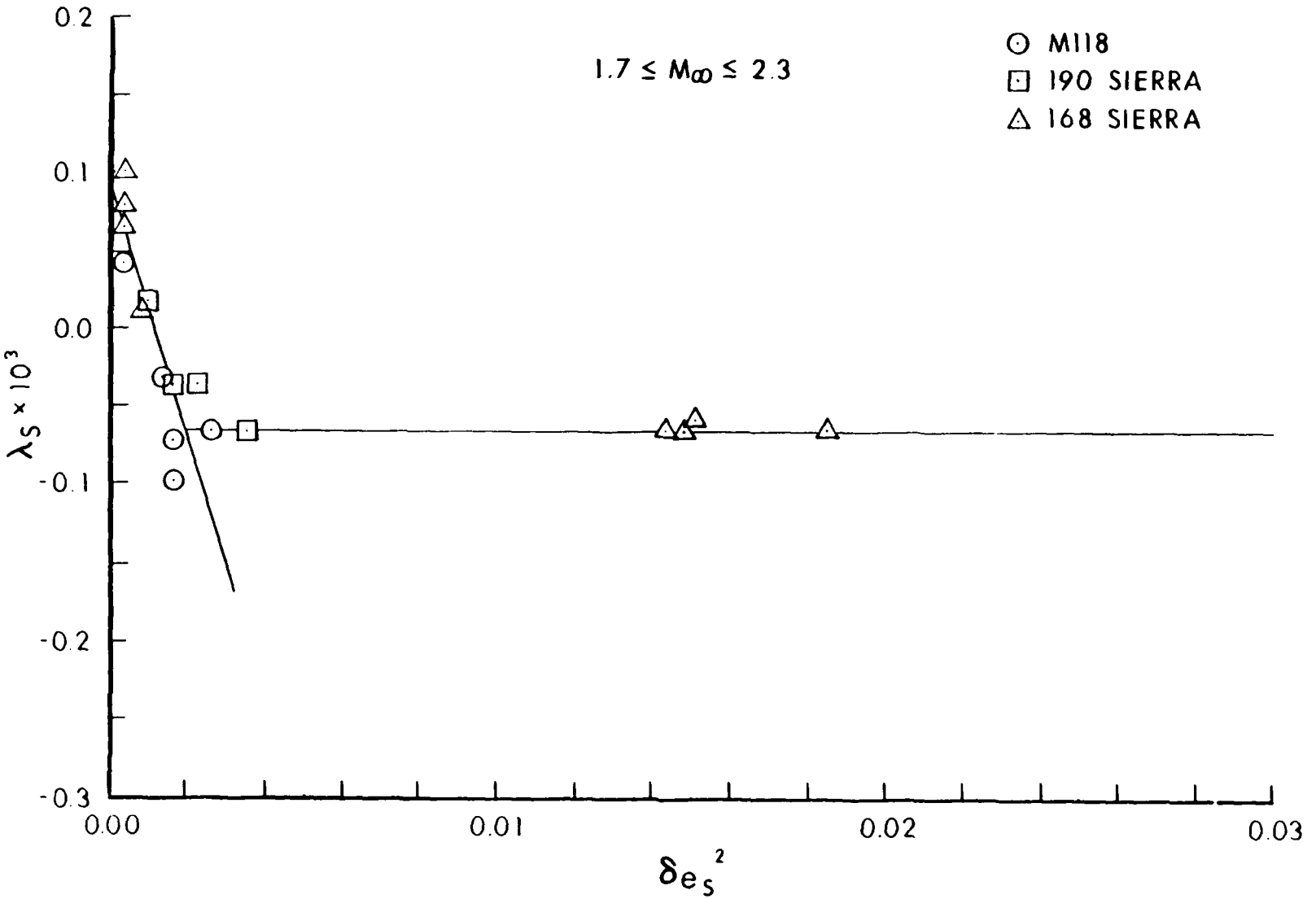

Figure 40. Slow Arm Damping Rate versus Effective Squared Yaw.

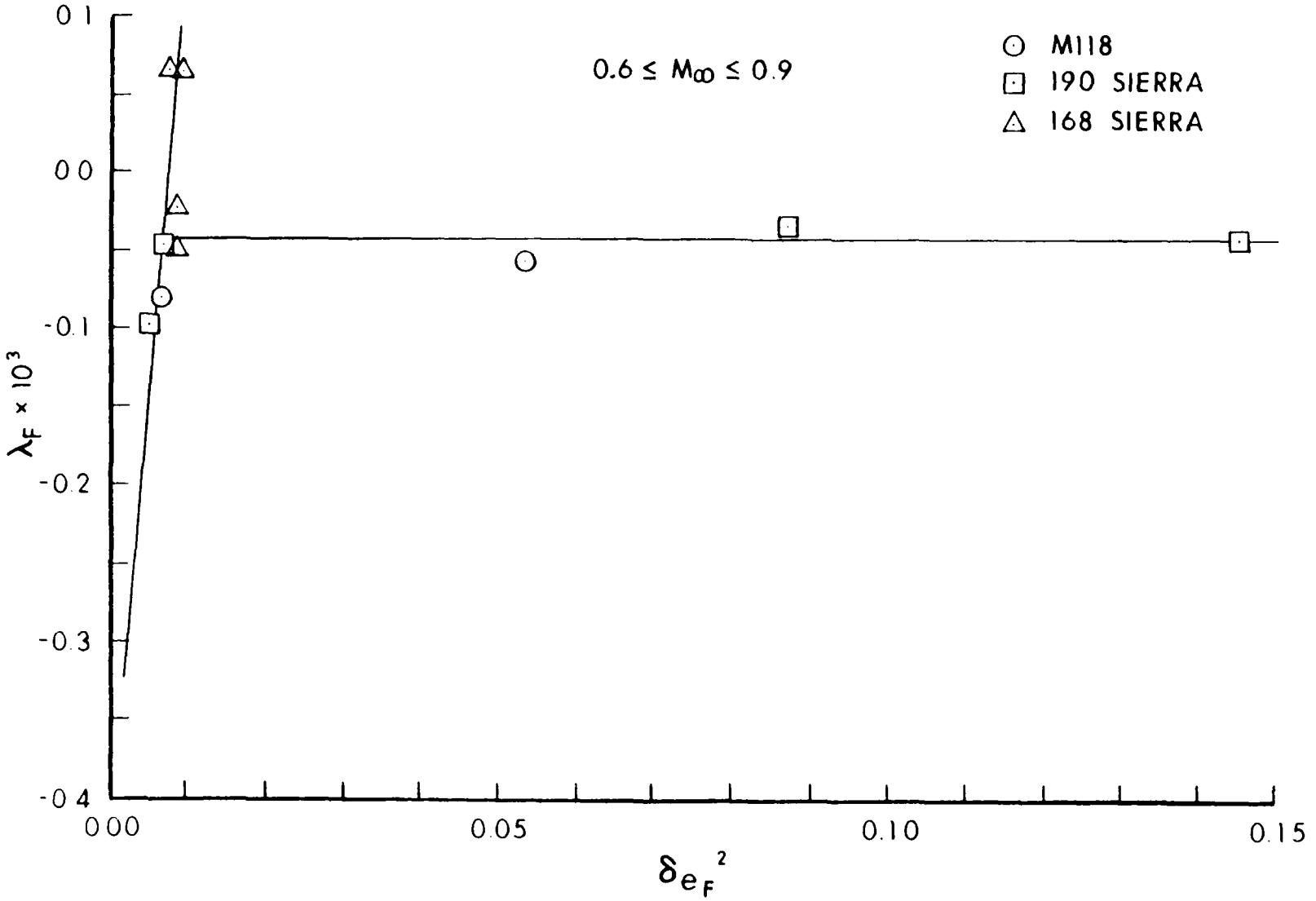

Figure 41. Fast Arm Damping Rate versus Effective Squared Yaw.

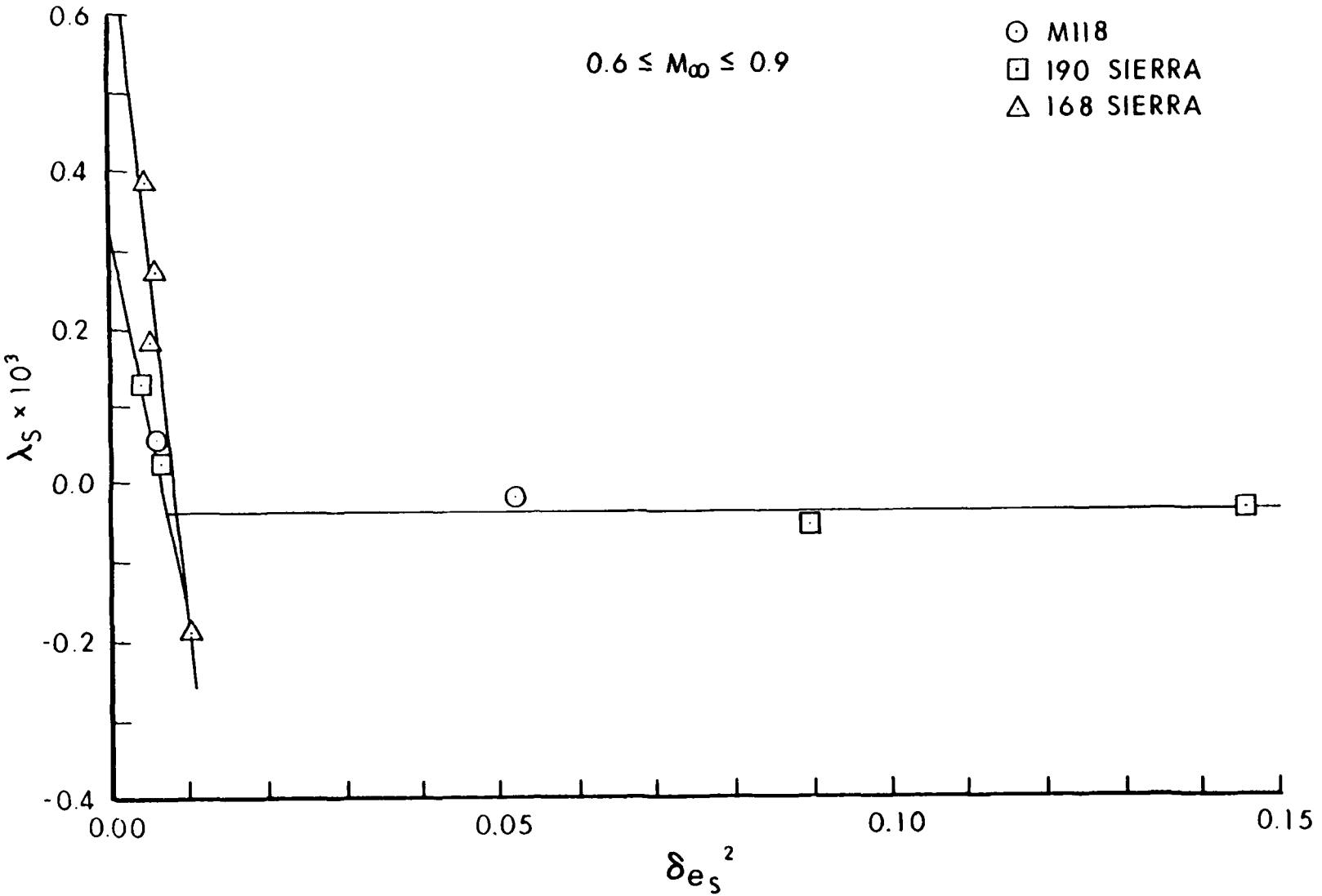

Figure 42. Slow Arm Damping Rate versus Effective Squared Yaw.

Table 1. Average Physical Characteristics of 7.62mm Match Bullets.

Projectile	Reference Diameter (mm)	Weight (grams)	Center of Gravity (cal - base)	Axial Moment of Inertia ($gm\text{-}cm^2$)	Transverse Moment of Inertia ($gm\text{-}cm^2$)
M118	7.82	11.27	1.80	.716	6.78
190 Sierra	7.82	12.27	1.81	.787	7.68
168 Sierra	7.82	10.89	1.54	.722	5.38

Table 2. Aerodynamic Characteristics of the M118 Match Bullet.

Round Number	Mach Number	α_t (degrees)	C_D	C_{M_α}	C_{L_α}	$C_{M_{p\alpha}}$	$(C_{M_q} + C_{M_\alpha})$	CP_N (cal - base)
13903	2.191	2.60	.3290	2.54	2.61	.10	-5.81	2.66
13901	2.184	2.03	.3263	2.57	2.60	.23	-6.87	2.68
13902	2.181	2.10	.3219	2.55	2.59	.13	-6.35	2.68
13906	1.848	1.01	.3361	2.78	--	-.17	-4.04	--
13907	1.801	1.93	.3436	2.72	--	.07	-5.99	--
13912	1.407	6.64	.4629	2.89	2.12	.32	-8.10	2.92
13911	1.395	2.20	.3907	2.98	2.37	-.12	-3.16	2.88
13918	1.098	3.22	.4326	3.18	1.72	-.35	1.47	3.27
13920	1.086	7.60	.4968	3.09	1.64	.16	-5.80	3.24
13929	.803	3.61	.1459	3.35	1.41	-.27	.14	3.95
13930	.798	10.80	.2425	3.16	1.47	-.01	-2.30	3.65

Table 3. Aerodynamic Characteristics of the 190 Grain Sierra Matchking Bullet.

Round Number	Mach Number	α_t (degrees)	C_D	C_{M_α}	C_{L_α}	$C_{M_{p\alpha}}$	$(C_{M_q} + C_{M_\alpha})$	CP_N (cal - base)
13904	2.208	1.43	.3306	2.82	--	-.02	-7.85	--
13905	2.138	3.25	.3411	2.83	3.02	.10	-6.95	2.65
13909	1.821	2.41	.3615	2.98	--	.05	-5.18	--
13908	1.800	2.11	.3560	2.96	2.41	.01	-5.62	2.88
13914	1.440	2.37	.3971	3.18	2.23	-.13	-5.53	3.02
13915	1.347	4.52	.4590	3.19	2.11	.16	-7.51	3.06
13922	1.140	4.23	.4588	3.33	1.93	.02	-5.12	3.20
13921	1.114	2.93	.4394	3.35	--	-.54	1.80	--
13935	.763	3.73	.1441	3.58	--	.05	-1.11	--
13933	.732	3.16	.1452	3.57	1.64	-.58	2.82	3.81
13934	.673	4.06	.2844	3.15	1.58	.15	-4.06	3.50
13931	.639	18.29	.3848	2.94	1.97	.03	-2.56	3.06

Table 4. Aerodynamic Characteristics of the 168 Grain Sierra International Bullet.

Round Number	Mach Number	α_t (degrees)	C_D	C_{M_α}	C_{L_α}	$C_{M_{p\alpha}}$	$(C_{M_q} + C_{M_\alpha})$	CP_N (cal - base)
12135	2.219	6.24	.3995	2.61	2.69	.10	-5.56	2.39
12130	2.217	1.63	.3404	2.69	--	-.17	-4.40	--
12129	2.210	1.04	.3371	2.66	--	-.23	-9.48	--
12136	2.202	6.95	.4099	2.62	2.69	.10	-5.55	2.39
12138	1.826	1.29	.3664	2.89	--	-.41	-6.09	--
12137	1.817	1.30	.3678	2.88	2.30	-.29	-9.22	2.62
12144	1.775	6.60	.4496	2.84	2.53	.11	-5.78	2.49
12145	1.773	6.81	.4503	2.84	2.49	.09	-5.83	2.51
12151	1.450	1.75	.4111	3.06	--	--	--	--
12152	1.412	2.08	.4182	3.06	2.02	-.37	-3.72	2.79
13924	1.150	7.79	.5451	3.00	1.88	-.06	-4.65	2.78
13923	1.119	1.79	.4433	2.99	--	--	--	--
13959	.866	4.12	.2033	3.17	--	-1.79	13.84	--
13939	.817	4.18	.1713	3.36	1.50	-1.41	13.60	3.55
13936	.753	3.73	.1592	3.35	1.39	-1.02	10.74	3.71
13941	.703	4.65	.1538	3.29	--	.66	-8.02	--

Table 5. Flight Motion Parameters of the M118 Match Bullet.

Round Number	Mach Number	S_g	S_d	$\lambda_F \times 10^3$ (1/cal)	$\lambda_S \times 10^3$ (1/cal)	K_F	K_S	o'_F (r/cal)	o'_S (r/cal)	Spin (r/cal)
13903	2.191	1.81	.84	-.106	-.065	.0276	.0316	.0161	.0032	.183
13901	2.184	1.79	1.02	-.095	-.098	.0229	.0232	.0161	.0032	.184
13902	2.181	1.77	.86	-.110	-.071	.0217	.0256	.0159	.0033	.181
13906	1.848	1.66	-.16	-.164	.042	.0041	.0166	.0160	.0036	.186
13907	1.801	1.61	.62	-.130	-.032	.0176	.0262	.0154	.0037	.181
13912	1.407	1.58	1.01	-.101	-.106	.0808	.0738	.0155	.0038	.183
13911	1.395	1.52	.46	-.108	-.007	.0172	.0332	.0152	.0040	.182
13918	1.098	1.39	--	-.060	.046	.0353	.0435	.0145	.0045	.180
13920	1.086	1.43	.85	-.092	-.062	.0920	.0955	.0147	.0043	.180
13929	.803	1.30	-2.01	-.078	.062	.0393	.0490	.0140	.0049	.179
13930	.798	1.38	.73	-.055	-.017	.1287	.1358	.0144	.0045	.179

Table 6. Flight Motion Parameters of the 190 Grain Sierra Matchking Bullet.

Round Number	Mach Number	S_g	S_d	$\lambda_F \times 10^3$ (1/cal)	$\lambda_S \times 10^3$ (1/cal)	K_F	K_S	ϕ'_F (r/cal)	ϕ'_S (r/cal)	Spin (r/cal)
13904	2.208	1.69	.30	-.171	.017	.0157	.0192	.0152	.0033	.181
13905	2.138	1.72	.82	-.118	-.067	.0313	.0412	.0156	.0033	.185
13909	1.821	1.61	.70	-.101	-.036	.0240	.0320	.0152	.0036	.184
13908	1.800	1.61	.65	-.119	-.034	.0180	.0300	.0152	.0036	.183
13914	1.440	1.54	.26	-.157	.014	.0143	.0372	.0150	.0038	.184
13915	1.347	1.54	.78	-.121	-.058	.0440	.0580	.0150	.0038	.184
13922	1.140	1.43	.61	-.113	-.022	.0475	.0560	.0143	.0042	.180
13921	1.114	1.42	-10.2	-.108	.092	.0294	.0414	.0143	.0042	.181
13935	.763	1.29	--	-.043	.029	.0440	.0478	.0134	.0048	.178
13933	.732	1.30	--	-.098	.134	.0316	.0444	.0136	.0047	.179
13934	.673	1.52	1.12	-.031	-.054	.1753	.1676	.0147	.0039	.181
13931	.639	1.68	1.05	-.040	-.033	.2179	.2253	.0154	.0034	.184

Table 7. Flight Motion Parameters of the 168 Grain Sierra International Bullet.

Round Number	Mach Number	S_g	S_d	$\lambda_F \times 10^3$ (1/cal)	$\lambda_S \times 10^3$ (1/cal)	K_F	K_S	ϕ'_F (r/cal)	ϕ'_S (r/cal)	Spin (r/cal)
12135	2.219	1.95	.76	-.134	-.066	.0622	.0836	.0194	.0035	.171
12130	2.217	1.92	.15	-.176	.016	.0091	.0258	.0195	.0036	.172
12129	2.210	1.88	.00	-.355	.064	.0017	.0172	.0191	.0036	.169
12136	2.202	1.94	.77	-.132	-.066	.0719	.0908	.0194	.0035	.171
12138	1.826	1.78	-.38	-.305	.102	.0014	.0206	.0191	.0039	.171
12137	1.817	1.78	-.05	-.365	.079	.0016	.0213	.0190	.0039	.171
12144	1.775	1.84	.75	-.138	-.065	.0571	.0882	.0194	.0038	.173
12145	1.773	1.84	.70	-.145	-.058	.0561	.0934	.0194	.0038	.173
12151	1.450	1.68	-.07	--	--	.0003	.0273	.0188	.0042	.171
12152	1.412	1.68	-.43	-.220	.079	.0044	.0339	.0187	.0042	.171
13924	1.150	1.89	.34	-.152	-.010	.0848	.1045	.0203	.0038	.180
13923	1.119	1.88	--	--	--	.0111	.0263	.0202	.0038	.179
13959	.866	1.68	--	-.021	.387	.0199	.0621	.0192	.0043	.175
13939	.817	1.61	--	.064	.271	.0260	.0644	.0189	.0045	.175
13936	.753	1.63	--	.066	.181	.0316	.0555	.0192	.0045	.176
13941	.703	1.64	1.33	-.047	-.187	.0648	.0473	.0191	.0044	.175

References

1. Braun, W.F., "The Free Flight Aerodynamics Range," US Army Ballistic Research Laboratory, Aberdeen Proving Ground, Maryland, BRL Report No. 1048, August 1958. (AD 202249)

2. Murphy C.H., "Data Reduction for the Free Flight Spark Ranges," US Army Ballistic Research Laboratory, Aberdeen Proving Ground, Maryland, BRL Report No. 900, February 1954. (AD 35833)

3. Murphy, C.H., "The Measurement of Non-Linear Forces and Moments by Means of Free Flight Tests," US Army Ballistic Research Laboratory, Aberdeen Proving Ground, Maryland, BRL Report No. 974, February 1956. (AD 93521)

4. Murphy, C.H, "Free Flight Motion of Symmetric Missiles," US Army Ballistic Research Laboratory, Aberdeen Proving Ground, Maryland, BRL Report No. 1216, July 1963. (AD 442757)

5. McCoy, R.L., "Aerodynamic and Flight Dynamic Characteristics of the New Family of 5.56mm NATO Ammunition," US Army Ballistic Research Laboratory, Aberdeen Proving Ground, Maryland, MR Report No. 3476, October 1985. (AD A162133)

List of Symbols

C_2	=	cubic static moment coefficient	
$\hat{C}_2$	=	cubic Magnus moment coefficient	
C_D	=	$\dfrac{\text{Drag Force}}{[(1/2)\rho V^2 S]}$	
C_{D_0}	=	zero-yaw drag coefficient	
$C_{D_{\delta^2}}$	=	quadratic yaw drag coefficient	
C_{L_α}	=	$\dfrac{\text{Lift Force}}{[(1/2)\rho V^2 S \delta]}$	Positive coefficient: Force in plane of total angle of attack. α_t, $\perp$ to trajectory in direction of α_t. (α_t directed from trajectory to missile axis.) $\delta = \sin\alpha_t$.
C_{N_α}	=	$\dfrac{\text{Normal Force}}{[(1/2)\rho V^2 S \delta]}$	Positive coefficient: Force in plane of total angle of attack. α_t, $\perp$ to missile axis in direction of α_t. $C_{N_\alpha} \cong C_{L_\alpha} + C_D$
C_{M_α}	=	$\dfrac{\text{Static Moment}}{[(1/2)\rho V^2 S d \delta]}$	Positive coefficient: Moment increases angle of attack α_t.
$C_{M_{p\alpha}}$	=	$\dfrac{\text{Magnus Moment}}{[(1/2)\rho V^2 S d\,(pd/V)\,\delta]}$	Positive coefficient: Moment rotates nose $\perp$ to plane of α_t in direction of spin.
$C_{N_{p\alpha}}$	=	$\dfrac{\text{Magnus Force}}{[(1/2)\rho V^2 S\,(pd/V)\,\delta]}$	Negative coefficient: Force acts in direction of 90° rotation of the positive lift force against spin.

List of Symbols (Continued)

For most exterior ballistic uses, where $\dot{\alpha} \approx q$, $\dot{\beta} \approx -r$, the definition of the damping moment sum is equivalent to:

$(C_{M_q} + C_{M_{\dot{\alpha}}})$	=	$\dfrac{\text{Damping Moment}}{[(1/2)\rho V^2 S d\,(q_t d/V)]}$	Positive coefficient: Moment increases angular velocity.
C_{l_p}	=	$\dfrac{\text{Roll Damping Moment}}{[(1/2)\rho V^2 S d\,(p d/V)]}$	Negative coefficient: Moment decreases rotational velocity.
C_{P_N}	=	center of pressure of the normal force, positive from base to nose	
α, β	=	angle of attack, side slip	
α_t	=	$(\alpha^2 + \beta^2)^{\frac{1}{2}} = \sin^{-1}\delta$, total angle of attack	
λ_F	=	fast mode damping rate	negative λ indicates damping
λ_S	=	slow mode damping rate	negative λ indicates damping
ρ	=	air density	
ω'_F	=	fast mode frequency	
ω'_S	=	slow mode frequency	
$c.m.$	=	center of mass	
d	=	body diameter of projectile, reference length	
d_2	=	cubic pitch damping moment coefficient	
I_x	=	axial moment of inertia	

List of Symbols (Continued)

I_y	=	transverse moment of inertia
K_F	=	magnitude of the fast yaw mode
K_S	=	magnitude of the slow yaw mode
l	=	length of projectile
m	=	mass of projectile
M	=	Mach number
p	=	roll rate
q, r	=	transverse angular velocities
q_t	=	$(q^2 + r^2)^{\frac{1}{2}}$
R	=	subscript denotes range value
s	=	dimensionless arc length along the trajectory
S	=	$(\pi d^2/4)$, reference area
S_d	=	dynamic stability factor
S_g	=	gyroscopic stability factor
V	=	velocity of projectile

List of Symbols (Continued)

Effective Squared Yaw Parameters

$$\tilde{\delta} \cong K_F^2 + K_S^2$$

$$\delta_e^2 = K_F^2 + K_S^2 + \frac{(\phi'_F K_F^2 - \phi'_S K_S^2)}{(\phi'_F - \phi'_S)}$$

$$\delta_{e_F}^2 = K_F^2 + 2K_S^2$$

$$\delta_{e_S}^2 = 2K_F^2 + K_S^2$$

$$\delta_{e_{HT}}^2 = \left(\frac{I_y}{I_x}\right)\left[\frac{(\phi'_F + \phi'_S)(K_S^2 - K_F^2)}{(\phi'_F - \phi'_S)}\right]$$

$$\delta_{e_{TH}}^2 = \left(\frac{I_x}{I_y}\right)\left[\frac{(K_F^2 \phi'^2_F - K_S^2 \phi'^2_S)}{(\phi'^2_F - \phi'^2_S)}\right]$$

$$\delta_{e_{HH}}^2 = \frac{(\phi'_F K_S^2 - \phi'_S K_F^2)}{(\phi'_F - \phi'_S)}$$

Distribution List

No. of Copies	Organization
12	Administrator Defense Technical Information Center ATTN: DTIC-DDA Cameron Station Alexandria, VA 22304-6145
1	HQDA (SARD-TR) Washington, DC 20310
1	Commander US Army Materiel Command ATTN: AMCDRA-ST 5001 Eisenhower Avenue Alexandria, VA 22333-0001
1	Commander US Army Laboratory Command ATTN: AMSLC-DL Adelphi, MD 20783-1145
1	Commander US Army Armament, Munitions and Chemical Command ATTN: AMCAR-ESP-L Rock Island, IL 61299-7300
1	Commander US Army Tank Automotive Command ATTN: AMSTA-TSL Warren, MI 48090
1	Commander US Army Communications - Electronics Command ATTN: AMSEL-ED Fort Monmouth, NJ 07703
1	Commander US Army Missile Command ATTN: AMSMI-RD Redstone Arsenal, AL 35898-5000
1	Commander US Army Missile Command ATTN: AMSMI-AS Redstone Arsenal, AL 35898-5500
1	Commander Armament Research, Development and Engineering Center US Army AMCCOM ATTN: SMCAR-MSI Picatinny Arsenal, NJ 07806-5000
1	Commander Armament Research, Development and Engineering Center US Army AMCCOM ATTN: SMCAR-TDC Picatinny Arsenal, NJ 07806-5000
1	Director Benet Weapons Laboratory Armament Research, Development and Engineering Center US Army AMCCOM ATTN: SMCAR-LCB-TL Watervliet, NY 12189
1	Director US Army TRADOC Analysis Command ATTN: ATAA-SL White Sands Missile Range, NM 88002

Distribution List (Continued)

No. of Copies	Organization
1	Commandant US Army Infantry School ATTN: ATSH-CD-CSO-OR Fort Benning, GA 31905-5400
1	Commander US Army Aviation Systems Command ATTN: AMSAV-DACL 4300 Goodfellow Blvd. St. Louis, MO 63120-1798
1	Director US Army Aviation Research and Technology Activity Ames Research Center Moffett Field, CA 94035-1099
1	Air Force Armament Laboratory ATTN: AFATL/DLODL Eglin AFB, FL 32542-5000
1	AFWL/SUL Kirtland AFB, NM 87117-6008
1	US Army JFK Center ATTN: ATSU-CD-ML Mr. S. Putnam Fort Bragg, NC 28307-5007
1	Commander US Army Materiel Command ATTN: AMXSO Mr. J. McKernan 5001 Eisenhower Avenue Alexandria, VA 22333-0001
1	Commandant US Army Infantry School ATTN: ATSH-CD Fort Benning, GA 31905-5400
1	President US Army Infantry Board ATTN: ATZB-IB-SA Mr. L. Tomlinson Fort Benning, GA 31905-5800
1	Commander Naval Sea Systems Command ATTN: Code 62CE Mr. R. Brown Washington, DC 20362-5101
4	Commanding Officer Naval Weapons Support Center ATTN: Code 2021, Bldg. 2521 Mr. C. Zeller ATTN: Code 2022 Mr. R. Henry Mr. G. Dormick Mr. J. Maassen Crane, IN 47522-5020
1	Commanding General MCDEC ATTN: Code D091 Fire Power Division Quantico, VA 22134-5080
1	US Secret Service J. J. Rowley Training Center ATTN: Mr. R. Lutz 9200 Powder Mill Road, RD 2 Laurel, MD 20707

Distribution List (Continued)

No. of Copies	Organization
14	Commander Armament Research, Development and Engineering Center US Army AMCCOM ATTN: SMCAR-SCJ Mr. J. Ackley Mr. V. Shisler Mr. H. Wreden Mr. J. Hill ATTN: SMCAR-CCL-AD Mr. F. Puzycki Mr. W. Schupp Mr. R. Mazeski Mr. D. Conway ATTN: SMCAR-CCL-FA Mr. R. Schlenner Mr. J. Fedewitz Mr. P. Wyluda ATTN: SMCAR-SCA-AP Mr. W. Bunting Mr. P. Errante ATTN: SMCAR-ATE-AP Mr. R. Kline Picatinny Arsenal, NJ 07806-5000

Aberdeen Proving Ground

Director, USAMSAA
ATTN: AMXSY-D
AMXSY-MP
Mr. H. Cohen
AMXSY-J
Mr. K. Jones
Mr. M. Carroll
Mr. J. Weaver
Mr. E. Heiss
AMXSY-GI
Mr. L. DeLattre

Commander, USATECOM
ATTN: AMSTE-TO-F

Cdr, CRDEC, AMCCOM
ATTN: SMCCR-MU
SMCCR-RSP-A
Mr. M. Miller
Mr. J. Huerta
SMCCR-SPS-IL

Director, USAHEL
ATTN: SLCHE-IS
Mr. B. Corona
Mr. P. Ellis

Director, USACSTA
ATTN: STECS-AS-LA
Mr. G. Niewenhous

USER EVALUATION SHEET/CHANGE OF ADDRESS

This laboratory undertakes a continuing effort to improve the quality of the reports it publishes. Your comments/answers below will aid us in our efforts.

1. Does this report satisfy a need? (Comment on purpose, related project, or other area of interest for which the report will be used.) _____

2. How, specifically, is the report being used? (Information source, design data, procedure, source of ideas, etc.) _____

3. Has the information in this report led to any quantitative savings as far as man-hours or dollars saved, operating costs avoided, or efficiencies achieved, etc? If so, please elaborate. _____

4. General Comments. What do you think should be changed to improve future reports? (Indicate changes to organization, technical content, format, etc.) _____

BRL Report Number _____ Division Symbol _____

Check here if desire to be removed from distribution list. ____

Check here for address change. ____

Current address: Organization _____
Address _____

----------FOLD AND TAPE CLOSED----------

Director
U.S. Army Ballistic Research Laboratory
ATTN: SLCBR-DD-T(NEI)
Aberdeen Proving Ground, MD 21005-5066

OFFICIAL BUSINESS
PENALTY FOR PRIVATE USE $300

BUSINESS REPLY LABEL
FIRST CLASS PERMIT NO. 12062 WASHINGTON D C

POSTAGE WILL BE PAID BY DEPARTMENT OF THE ARMY

NO POSTAGE NECESSARY IF MAILED IN THE UNITED STATES

Director
U.S. Army Ballistic Research Laboratory
ATTN: SLCBR-DD-T(NEI)
Aberdeen Proving Ground, MD 21005-9989